Applied Environmental Microbiology

The coral pathogen *Vibrio coralliilyticus* utilizes the compatible solute and signaling molecule *myo*-inositol as a sole carbon source

Katherine E. Boas Lichty and E. Fidelma Boyd

Department of Biological Sciences, University of Delaware

Abstract. Marine bacteria experience fluctuations in osmolarity that they must adapt to, and most bacteria respond to high osmolarity by accumulating compatible solutes. The osmotic stress response and compatible solutes used by the marine pathogen *Vibrio coralliilyticus* are unknown. In this study, we showed that to alleviate osmotic stress *V. coralliilyticus* biosynthesized the compatible solute glycine betaine (GB) and transported choline, GB, ectoine, dimethylglycine, and dimethylsulfoniopropionate, for osmoprotection, but not *myo*-inositol. *Myo*-inositol is a stress protectant and a signaling molecule that is biosynthesized by algae. Bioinformatics analysis identified two contiguous *myo*-inositol metabolic gene clusters in all *V. coralliilyticus* genomes. Growth pattern analysis demonstrated that *V. coralliilyticus* utilized *myo*-inositol as a sole carbon source, with a short 3 h lag time, and the inositol 2-dehydrogenase (*iolG)* gene was required for this growth. Genetic analysis identified both an MFS-type (IolT1) and ABC-type (IolXYZ) transporter in the metabolic gene clusters that transported *myo*-inositol. Further genomics and phylogenetic analyses showed that the *myo*-inositol metabolic gene clusters were widespread among *Vibrionaceae* (*Vibrio, Photobacterium, Enterovibrio,* and *Grimontia* species) and acquired several times within the group. IolG was most closely related to IolG from *Aeromonas, Pectobacterium (*formerly *Erwinia),* and *Dickeya* species. These species contained the *iol* genes in a single metabolic gene cluster with an *iolXYZ* transporter. In *Aeromonas*, the cluster was always found within mobile genetic elements, but present only in a few species, predominantly in strains of *A. hydrophila* and *A. dhakensis*.

Importance. Bacterial pathogens such as *V. coralliilyticus* encounter competition for nutrient sources and have evolved metabolic strategies to adapt to nutrient opportunities. Emerging studies show that *myo*-inositol is exchanged in the coral-algae symbiosis, likely involved in signaling, but is also a compatible solute in algae. Our findings that the coral pathogens *V. coralliilyticus* and *V. mediterranei* contained *myo*-

inositol metabolism gene clusters suggest this could be an important adaptation. The consumption of *myo*-inositol by these coral pathogens could contribute to a breakdown of the coral-algae symbiosis by inhibition of algal survival or algal expulsion leading to coral bleaching. Phylogenetic analysis showed that a *myo*-inositol metabolism gene cluster is ancestral to *Pectobacterium* and *Dickeya*, but was acquired recently by horizontal gene transfer in hypervirulent strains of *Aeromonas*.

Introduction

Vibrio coralliilyticus is a Gram-negative rod-shaped marine bacterium, a member of the family *Vibrionaceae*, and important pathogen of coral and larval oysters. This species was first characterized as the etiological agent for coral bleaching of *Pocillopora damicornis*, and has since been identified as a pathogen in numerous other species of coral (1-16). Recent studies also have shown that *V. coralliilyticus* and a related species *V. tubiashii* cause high mortalities in oyster larvae of both Pacific oyster (*Crassostrea gigas*) and Eastern oyster (*Crassostrea virginica*) in the United States (6, 17-22).

Under homeostatic conditions, the relationship between *V. coralliilyticus* and *P. damicornis* is commensal (23-25). However, with increased temperatures the abundance of *V. coralliilyticus* expands, and this in addition to other factors can turn the relationship pathogenic (26-34). One route of pathogenesis is the expulsion of the corals' endosymbiotic dinoflagellate algae (genus *Symbiodinium*) that occurs with increased *V. coralliilyticus* abundance (2, 12, 26, 27, 35, 36). Dinoflagellate algae cells are given protection and live intracellularly within coral cells, while providing their coral host with metabolites as a reliable food source (37-42). Corals thrive because of this mutualistic symbiosis with dinoflagellate algae and central to maintaining this relationship is metabolic exchange (43-48).

One metabolite exchanged between dinoflagellate algae and coral is *myo*-inositol (38, 39, 49). While the function of *myo*-inositol is not yet established in the coral-algae symbiosis, this compound is known to be biosynthesized by algae (43, 50, 51) and hypothesized to be transported to coral (39, 52). *Myo*-inositol is a six-carbon polyol compound and the most abundant form of inositol in the environment (53-55). In response to increased salinity; algae, plants, and marine invertebrates use *myo*-inositol as a compatible solute for osmotic stress protection to maintain cellular turgor pressure

72 (56-58). Additionally, in algae and plants, *myo*-inositol has been implicated as an
73 important signaling molecule (49, 59-61).

74 Studies have shown that soil bacteria and human bacterial pathogens can utilize
75 *myo*-inositol as an energy source (62, 63). Genetics and enzyme functionality studies for
76 bacterial *myo*-inositol catabolism genes was first established and investigated in Gram-
77 positive *Bacillus subtilis* (64-67) (**Fig. 1**). *Myo*-inositol is degraded by inositol 2-
78 dehydrogenase (IolG) into 2-keto-*myo*-inositol, which is then converted by myo-inosose
79 dehydratase (IolE) to 3,5/4-Trihydroxycylohexane-1,2-dione. This is subsequently
80 hydrolyzed into 5-deoxy-D-gluconate by the acylhydrolase (IolD). This product is then
81 isomerized by 5-deoxy-glucuronate isomerase (IolB) and phosphorylated by 5-dehydro-
82 2-deoxygluconokinase (IolC). Then 2-deoxy-5-keto-D-gluconate-6-P is converted to
83 dihydroxyacetone (DHA) and malonate semialdehyde by an aldolase (IolJ). Malonate
84 semialdehyde is converted to acetyl-CoA by the CoA-acylating methylmalonate-
85 semialdehyde dehydrogenase (IolA). The product DHA can enter glycolysis and acetyl-
86 CoA can enter the TCA cycle (65-68). The transport of *myo*-inositol into *B. subtilis* for
87 catabolism is performed by two major facilitator superfamily (MFS)-type transporters,
88 named IolT and IolF (65). Several Gram-negative bacteria have been shown to use *myo*-
89 inositol as a metabolite with a similar pathway, species in the genera *Klebsiella,*
90 *Caulobacter, Rhizobium, Sinorhizobium, Pseudomonas, Yersinia, Corynebacterium, Salmonella*,
91 and *Serratia* (69-78). For example, the human pathogen *Salmonella enterica* serovar
92 Typhymurium utilized *myo*-inositol as a sole carbon source, but growth on *myo*-inositol
93 was characterized by a long lag phase of > 45 h and a bistable phenotype (63, 71, 72, 79,
94 80). This species was found to use two MFS family transporters, named IolT1 and IolT2
95 for *myo*-inositol uptake (72). In the Alpha-proteobacteria *Caulobacter vibrioides* (formerly
96 *crescentus*) catabolism of *myo*-inositol was demonstrated and uptake was shown by an

97 ABC-type transporter (70, 81). *Myo*-inositol utilization has not been previously
98 examined in marine bacteria.

99 Here, we established the osmotic stress response of *V. coralliilyticus* at different
100 temperatures and showed a salinity growth range between 1% NaCl to 4% NaCl with
101 optimal growth in 2% NaCl at 28°C. Bioinformatics analysis of the genomes of *V.*
102 *coralliilyticus* identified the genes required for the biosynthesis of glycine betaine (GB)
103 and homologs of six compatible solute transporters. Our work determined that *V.*
104 *coralliilyticus* can uptake a range of compatible solutes for osmotic protection and
105 showed that GB can be biosynthesized from choline. Our analysis also identified a large
106 genomic region containing two distinct metabolic gene clusters with homologs of genes
107 for the regulation, transport, and catabolism of *myo*-inositol. Growth pattern analysis
108 demonstrated that *V. coralliilyticus* isolates used *myo*-inositol as a sole carbon source. We
109 also provided experimental evidence that these metabolic regions are required for
110 transport and catabolism of *myo*-inositol. Comparative genomics and phylogenetic
111 analyses demonstrated that the two gene clusters were acquired independently among
112 closely related species of the family *Vibrionaceae*. IolG from *Vibrio* species was most
113 closely related to IolG from *Aeromonas, Dickeya,* and *Pectobacterium* species. Within each
114 of these genera, the *iol* genes were present in a single cluster and were highly related to
115 one another except for the *Aeromonas* species. In this group the cluster was divergent
116 among species and present on a mobile genetic element indicative of recent horizontal
117 transfer into this genus.

118 **Results**

119 ***Vibrio coralliilyticus* has a relatively narrow salinity range compared to other *Vibrio***
120 ***species.*** Previous work has shown that several *Vibrio* species can grow in 1% to 7%
121 NaCl without the addition of compatible solutes (82-87). To establish the ability of *V.*
122 *coralliilyticus* to thrive in a range of NaCl concentrations, we examined growth patterns

123 in M9 minimal media supplemented with glucose (M9G) and 1% to 5% NaCl at 21°C,
124 28°C 34°C and 37°C for 24 h (**Fig. 2**). Under all the conditions tested, *V. coralliilyticus*
125 grew optimally in M9G 2% NaCl at 28°C (**Fig. 2A**). At this temperature, the final OD
126 was 0.81 in 2% NaCl whereas in 1% NaCl, the final OD reached was 0.47. When the
127 salinity was increased to 3% NaCl the maximum growth rate and area under the curve
128 (0.66 h^{-1}, 15.3) were lower than what was observed at 2% NaCl (0.76 h^{-1}, 16.5). Growth of
129 *V. coralliilyticus* in 4% NaCl showed 2 h lag time and lower maximum growth rate (0.40
130 h^{-1}) whereas no growth occurred in 5% NaCl (**Fig. 2A**). Next, we tested whether
131 temperature affected the salinity growth range by examining growth at 21°C, 34°C and
132 37°C (**Fig. 2B-D**). Two observations were made from these analyses; first incubation at
133 21°C negatively affected growth in 4% NaCl resulting in a significantly longer lag phase
134 than at any other temperature (**Fig. 2B**). Secondly, incubation at 37°C impacted the
135 ability to grow in low salinity; at this temperature there was no growth in 1% NaCl (**Fig.
136 2D**). Overall, growth in 1% NaCl at 28°C, 34°C and 37°C resulted in a final OD lower
137 than what was observed at the higher NaCl concentrations up to 4% NaCl (**Fig. 2**).

138 ***V. coralliilyticus* biosynthesizes glycine betaine (GB) and uptakes numerous
139 compatible solutes for osmotic protection.** Analysis of *V. coralliilyticus* genomes
140 identified a gene cluster involved in the biosynthesis of GB from the precursor choline
141 (*betIBA*) and six putative compatible solute transporters (**Fig. 3A**). ^{1}H-NMR spectra
142 analysis of ethanol extracts for *V. coralliilyticus* grown in M9G 4% NaCl supplemented
143 with 1 mM choline confirmed glycine betaine biosynthesis (**Fig. 3B**). To establish the
144 range of compatible solutes taken up by *V. coralliilyticus* for osmotic protection, cells
145 were grown in M9G 5% NaCl supplemented with one of ten different compatible
146 solutes. The growth pattern in each compatible solute was monitored for 24 h at 28°C.
147 Seven of the ten compatible solutes tested restored growth (**Table 1**). GB,
148 dimethylsulfoniopropionate (DMSP), ectoine, choline, and dimethylglycine (DMG)

149 rescued growth to the greatest extent reaching a final OD ranging from 0.45 to 0.69
150 (**Table 1**). The compatible solutes γ-amino-butyric acid (GABA) and creatine had longer
151 lag phase times and reached a final OD of 0.23 and 0.31, respectively (**Table 1**).
152 Trimethylamine-N-oxide, *myo*-inositol (MI), and glycerol were unable to rescue growth
153 of *V. coralliilyticus* in M9G 5% NaCl indicating they are not used for osmotic protection
154 in this species (**Table 1**).

155 ***Myo*-inositol metabolic gene clusters are present in all strains of the coral pathogens**
156 ***V. coralliilyticus* and *V. mediterranei*.** Bioinformatics analysis identified putative *myo*-
157 inositol metabolic gene clusters that were present in all *V. coralliilyticus* genomes
158 examined. The region contained two distinct gene clusters for the regulation, transport,
159 and catabolism of *myo*-inositol (**Fig. 4**), named region 1 and region 2. Gene annotation
160 and naming were established based upon amino acid similarity to *Salmonella enterica*.
161 The gene clusters and gene order were highly conserved among *Vibrio* species. No
162 synteny was found between *myo*-inositol gene clusters in *Vibrio* species and *S. enterica,*
163 *B. subtilis,* or *C. vibrioides* (**Fig.4**). Functionally similar genes present in region 1 and
164 region 2 in *V. coralliilyticus* shared low sequence similarity (27% to 50%) and lacked
165 gene synteny.

166 Region 1 contained fifteen genes, which included a predicted operon composed
167 of ten genes *iolEDOCBJRIBG* encoding putative enzymes responsible for *myo*-inositol
168 conversion to dihydroxyacetone and malonate semialdehyde (**Fig.4**). Region 1 also
169 contained two MFS transporters, a LysR family transcriptional regulator, a
170 glycosyltransferase and a polysaccharide biosynthesis protein. A single copy of the *iolG*
171 gene (inositol 2-dehydrogenase) was present in the metabolic gene clusters, this enzyme
172 is required for the first step in the pathway (**Fig. 1**). IolG shares 36.1% amino acid
173 identity to IolG2 from *S. enterica* (**Fig.4**). A copy of *iolE* and *iolD* are present within
174 region 1 and encode enzymes involved in the second and third steps of the catabolic

175 pathway. Two copies of IolE and IolD are present, a copy in each region. Region 1
176 copies are named IolE2 and IolD2 as they share only 38% amino acid identity to the
177 enzymes from *S. enterica* (**Fig.4**). A putative 5-dehydro-2-deoxyglucokinase is encoded
178 by *iolC* is also found in region 1 and shares 33% amino acid identify with IolC from *S.*
179 *enterica*. The next step in the pathway is completed by an oxidoreductase encoded by
180 *iolB*; two copies of this gene were found in region 1 (IolB1 and IolB2), sharing 63.5% and
181 31% amino acid identify to IolB from *S. enterica* (**Fig. 4**). Region 1 also contained a
182 hypothetical Gfo/Idh/MocA family oxidoreductase that we named *iolO*.

183 Region 2 contained a predicted operon *iolCDEA*, which overall shared greater
184 amino acid identity ranging from 67.4% to 43.7% with proteins from *S. enterica* (**Fig.4**).
185 In region 2, an *iolA* homolog shared 65.2% amino acid identity to IolA from *S. enterica*
186 and encoded a CoA-acylating methylmalonate-semialdehyde dehydrogenase involved
187 in the conversion of malonate semialdehyde to acetyl-CoA. There is no homolog for
188 IolA in region 1. The *iolCDE* genes were named *iolC1D1E1* as they share the closest
189 homology to proteins in *S. enterica*. Divergently transcribed from this operon is the
190 putative operon *iolXYZR* that encodes an ABC-type transporter IolXYZ and an RpiR
191 type regulator IolR (**Fig.4**). *S. enterica* does not possess an ABC-type transporter that
192 uptakes *myo*-inositol therefore this transporter was compared to another Gram-negative
193 species known to transport *myo*-inositol for catabolism. The substrate binding protein
194 IolX from *V. coralliilyticus* shares 31% amino acid identity with IbpA a known
195 transporter of *myo*-inositol in *Caulobacter vibrioides* (81).

196 A similar gene arrangement in region 1 was present in the genomes of the coral
197 pathogen *V. mediterranei* (formerly *V. shilonii*) and related species *V. maritimus* and *V.*
198 *barjaei* (**Fig.4**). However, in these species region 1 was contiguous with region 2, and this
199 cluster contained the operon *iolCA* divergently transcribed from *iolXYZR* (**Fig.4**).

200 ***V. coralliilyticus* can utilize *myo*-inositol as a sole carbon source.** To demonstrate *myo*-
201 inositol catabolism by *V. coralliilyticus*, strain CN52H-1 was grown in M9 2% NaCl
202 media supplemented with 20 mM Glucose or 20mM *myo*-inositol as carbon sources at
203 28°C for 30 h. *V. coralliilyticus* growth in M9 2% NaCl with 20mM *myo*-inositol reached a
204 final OD of 0.29 with a lag time of 3 h (**Fig. 5A**). We also examined *V. harveyi* growth, a
205 species that contains region 1, but not region 2, and found that this species grew in
206 glucose but did not grow in *myo*-inositol as a sole carbon source (**Fig. 5B**). This
207 suggested that region 2 is essential for *myo*-inositol catabolism. To demonstrate that
208 region 1 is also required for *myo*-inositol catabolism, an in-frame deletion of *V.*
209 *coralliilyticus iolG* (HRJ43_RS06535) was generated and the Δ*iolG* strain showed no
210 growth in M9 2% NaCl media supplemented with 20 mM *myo*-inositol (**Fig. 5C**).
211 Overall, the data showed that *V. coralliilyticus* has a functioning *myo*-inositol pathway
212 and both region 1 and region 2 are required for catabolism in *Vibrio* species.

213 **Ligand modeling predicts *V. coralliilyticus* IolT1 and IolXYZ are *myo*-inositol**
214 **transporters**. Three transporters, two MFS-type transporters named IolT1 and IolT2
215 within region 1 and one ABC-type transporter IolXYZ within region 2 were identified.
216 Ligand modeling was performed to predict which of these are likely responsible for
217 *myo*-inositol transport by comparison to known transporters of *myo*-inositol. The MFS
218 transporters from *B. subtilis* IolT (WP_003234027.1) and *S. enterica* IolT1 (NP_463279.1)
219 were selected as these previously showed transport of *myo*-inositol (65). *V. coralliilyticus*
220 IolT1 (WP_099607352.1) had 48.8% amino acid identity to that of *S. enterica* IolT1
221 whereas *V. coralliilyticus* IolT2 (WP_172853823.1) shared only 27% similarity. Docking of
222 *myo*-inositol with *B. subtilis* IolT and *S. enterica* IolT1 predicted a mode of interaction
223 with seven and five putative binding residues, respectively and favorable binding free
224 energy changes (ΔG) of -7.0 kcal/mol and -6.1 kcal/mol. *Myo*-inositol docking with *V.*
225 *coralliilyticus* IolT1 predicted a favorable ΔG of -6.2 kcal/mol and four putative binding

226 residues. Alignment of *B. subtilis* IolT, *S. enterica* IolT1, *V. coralliilyticus* IolT1 and IolT2
227 was performed and predicted transmembrane domains are shown (**Fig. 6A**). MFS-type
228 transporters are known to coordinate substrate binding with transmembrane (TM)
229 domains TM7 and TM10 (88). Predicted binding residues found in the three models are
230 shown with blue (*V. coralliilyticus* IolT1), green (*S. enterica* IolT1), and orange (*B. subtilis*
231 IolT) arrows. (**Fig. 6B**). The two glutamine (Q273, Q274) and asparagine (N279) in TM7
232 are found in all three modeled sequences. In TM10 three of the four sequences also
233 contained a conserved tryptophan (W377) residue. All three models predicted a residue
234 that aligns at Y368. Both *V. coralliilyticus* IolT1 and *S. enterica* IolT1 contain a conserved
235 tyrosine (Y) residue here, but *B. subtilis* IolT contained glutamine (Q) (**Fig. 6A**). Taken
236 together this similarity in the binding pockets of these transporters suggested that *V.*
237 *coralliilyticus* IolT1 is likely able to transport *myo*-inositol.

238 The ABC-type transporter substrate binding protein IbpA from *C. vibrioides* had
239 previously been shown to bind *myo*-inositol (81) and IolX (WP_227495657.1) from *V.*
240 *coralliilyticus* had 87% coverage, 31% amino acid identity to IbpA. Ligand docking
241 analysis of *myo*-inositol with IbpA and IolX predicted favorable modes of action with
242 ΔG of -7.4 kcal/mol and -5.3 kcal/mol respectively. Putative binding residues were
243 identified for each substrate binding protein and are presented in the amino acid
244 alignment (**Fig. 6B**). The green arrows indicate IbpA predicted binding residues and
245 blue arrows indicate IolX predicted binding residues. Five aligned residues were
246 predicted to be important in both docking models: 63 aspartic acid (D)/ glutamine (Q),
247 141 aspartic acid (D)/ asparagine (N), 187 glutamine (Q)/ serine (S), 269 aspartic acid
248 (D), and 289 glutamine (Q) (**Fig. 6B**). Based upon the favorable docking model and
249 select conserved residues in the alignment with a known *myo*-inositol transporter,
250 IolXYZ is predicted to be capable of *myo*-inositol transport.

251 **The MFS transporter IolT1 and ABC-type transporter IolXYZ are responsible for**
252 ***myo*-inositol uptake for catabolism**. To evaluate the ability of IolT1 and IolXYZ to
253 transport *myo*-inositol, in-frame deletion mutants were generated in the *iolT1*
254 (HRJ43_RS06585) and *iolX (HRJ43_RS06670)* genes. The Δ*iolT1* mutant grew in *myo*-
255 inositol as the sole carbon source with a lag time of 6 h compared to wild type with a
256 lag time of 3 h and decreased maximum growth rate (Δ*iolT1;* 0.11 h^{-1}, wild type; 0.29 h^{-1})
257 (**Fig. 7**). Additionally, Δ*iolT1* reached a lower final OD (0.12) as compared to wild type
258 (0.29) (**Fig. 7**). This data indicated that IolT1 is utilized for the transport of *myo*-inositol,
259 but another transporter also uptakes this compound. Similarly, the growth pattern
260 analysis of the Δ*iolX* mutant showed growth in *myo*-inositol with a final OD of 0.17
261 compared to an OD of 0.29 in wild type (**Fig. 7**). *V. coralliilyticus* Δ*iolX* displayed a
262 maximum growth rate of 0.10 h^{-1} as compared to 0.29 h^{-1} observed for wild type (**Fig. 7**).
263 These data suggested IolXYZ also transported *myo*-inositol. Next, we constructed a
264 double mutant Δ*iolT1*/Δ*iolX* to determine whether any other transporters could uptake
265 *myo*-inositol. The double mutant failed to grow in M9 supplemented with *myo*-inositol
266 as a sole carbon source and demonstrated that *V. coralliilyticus* has two transporters for
267 *myo*-inositol uptake for catabolism (**Fig. 7**).

268 **Phylogenetic analysis of IolG from region 1 and IolA from region 2 among**
269 ***Vibrionaceae* reveals different evolutionary histories.** The low sequence similarity
270 between comparable proteins in each of the metabolic gene clusters and lack of synteny
271 suggested different evolutionary histories of these regions. To examine this further, a
272 phylogeny based on the IolG protein from region 1 was constructed among members of
273 the family *Vibrionaceae* (**Fig. 8**). In addition, a phylogeny based on the housekeeping
274 protein RpoB was also constructed among the same set of species to represent their
275 ancestral relationships (**Fig. 9**). BLAST analysis was performed using IolG
276 (WP_038162996.1), the inositol-2-dehydrogenase from region 1, as a seed to identify

277 protein sequences in the NCBI genome database. Sequences with >95% query coverage
278 and >60% amino acid similarity were downloaded and aligned using CLUSTALW (89).
279 The genome context of these IolG proteins within each species was determined and all
280 IolG proteins showed the presence of additional *myo*-inositol metabolism genes.
281 Phylogenetic trees were constructed, and a representative tree is presented in **Figure**
282 **8A**. IolG was present in *Vibrio* (red), *Photobacterium* (blue), *Enterovibrio* (orange), and
283 *Grimontia* (brown) species. Among *Vibrio* species, the IolG proteins are found dispersed
284 within three major branches on the tree. The *V. coralliilyticus* IolG clustered divergently
285 from members of the Mediterranei clade (**Fig. 8A**). Comparative genomics showed that
286 in the Mediterranei group region 1 was contiguous with region 2 whereas in *V.*
287 *coralliilyticus* the regions were separated by between 6 kb to 28 kb depending on the
288 strain. Branching distantly from these species were a highly similar cluster of IolG
289 proteins indicated by short branch lengths with species in the Harveyi clade. Within
290 this tight cluster was IolG from *V. vulnificus*, a species which is not a member of the
291 Harveyi clade. These data indicated that IolG and by extension region 1 were acquired
292 by horizontal gene transfer in *V. vulnificus* from a *Vibrio* species, region 2 was absent
293 among these species (**Fig. 8B**). The second major clustering of IolG from *Vibrio* species
294 contained long-branch lengths and relatively low bootstrap values. In this group, IolG
295 from *V. kanaloae, V. toranzoniae,* and *V. rumoiensis* clustered together. Branched distantly
296 from this group were IolG from two *Photobacterium* species that clustered divergently
297 from *V. anguillarum, V. ponticus,* and *V. metschnikovii* (**Fig. 8**). The *myo*-inositol gene
298 clusters in these species shared a similar gene order comprised of *iolDCEA* contiguous
299 with *iolB*, *iolR*, *iolG*, and *iolXYZ*, which differed significantly from the gene order
300 present in all other *Vibrio* species (**Fig. 8B**). The third cluster of IolG proteins from *Vibrio*
301 species contained IolG from four members of the Splendidus clade, which branched
302 divergently from IolG in nine *Photobacterium* species (**Fig. 8**). These all contained a
303 similar region 1 as the Harveyi clade, but region 2 showed different gene contents (**Fig.**

304 **8B**). The IolG proteins from five *Grimontia* species clustered closely together with short
305 branch lengths and grouped with IolG from *Enterovibrio calviensis and E. norvegicus* (**Fig.**
306 **8**). IolG was also present in four additional *Enterovibrio* species, branched separately
307 from the other two *Enterovibrio* species. Lastly, we observed *V. penaeicida* and *V.*
308 *nigripulchritudo* clustering divergently from the *Enterovibrio* and *Grimontia* groups.

309 The IolA protein, a CoA-acylating methylmalonate-semialdehyde
310 dehydrogenase, was selected as the representative of region 2 and used as a seed for
311 BLAST analysis. Eight *Vibrio* species that contained IolG did not have a copy of IolA or
312 any of the duplicate proteins present in region 2. These included species from the
313 Harveyi clade, *V. harveyi, V. campbellii, V. owensii,* and *V. jasicida*, as well as *V. astriarenae,*
314 *V. agarivorans, V. ponticus*, and *V. vulnificus*. In the IolA tree, the bootstrap values for
315 internal branch nodes for most *Vibrio* and *Photobacterium* species was low and indicated
316 that the relationships of IolA from these species is not clear (**Fig. 9**). In contrast, the
317 bootstrap values for IolA from *Grimontia* species were robust with short branch lengths
318 and indicated that they are highly related (**Fig. 9**). Branched divergently from these
319 were IolA from *Enterovibrio* species with greater than 85% confidence in many external
320 nodes and IolA from *V. penaeicida* and *V. nigripulchritudo* also clustered distantly within
321 this group (**Fig. 9**). The position of IolA from *Photobacterium* species within the tree
322 could not be determined as the internal bootstrap values were < 40%. In most *Vibrio*
323 species, we observed divergent branches with long-branch lengths, which represented
324 low IolA similarity to each other and a polyphyletic origin for IolA. The IolA protein
325 from *Photobacterium chitinilyticum,* but not *P. atrarenae,* similar to the IolG phylogeny,
326 branched distantly with IolA from *Vibrio* species.

327 The differences between the IolG and IolA trees and the comparative genomic
328 analysis showed that the two regions were acquired separately likely via horizontal
329 transfer, each with a different origin and ancestral history. Overall, the data suggested a

330 polyphyletic origin for the *myo*-inositol metabolic gene clusters and that a similar region
331 1 was acquired by *Vibrio* and *Photobacterium* species. Whereas a separate unrelated
332 region 1 was acquired by *Grimontia* and *Enterovibrio* species and a handful of *Vibrio*
333 species. The data also showed that when a region was present in a species, it was
334 present in all representatives of that species in the NCBI genome database. In addition,
335 there were no signatures of recent horizontal transfer such as the presence of IS
336 elements, transposases, integrases, phage, or plasmid elements within 10 genes of the
337 metabolic gene clusters.

338 To examine *myo*-inositol evolutionary history further, an IolG tree was
339 constructed from species outside of the *Vibrionaceae* family (**Fig. 10**). Within this tree,
340 IolG from *Vibrio* species clustered most closely with members of the genera *Aeromonas*,
341 *Pectobacterium (formerly Erwinia species),* and *Dickeya* with each genus tightly clustered
342 within distinct clades (**Fig. 10**). Genomic analysis of *Pectobacterium (formerly Erwinia),*
343 and *Dickeya* showed that the *myo*-inositol metabolic genes were present in a single
344 cluster; in *Pectobacterium* the operon structure was *iolADGXYZOCEB* with the ABC-type
345 transporter. In *Dickeya* species, the region was similar to what was seen in
346 *Pectobacterium* with the exception of three genes inserted between *iolD* and *iolG*. For
347 both these genera, IolG showed short branch lengths indicating these proteins are
348 highly related to one another within each genus. In six *Aeromonas* species, the
349 distribution and divergence of the region and proteins suggested the *iol* cluster was
350 acquired via horizontal gene transfer. The *iol* metabolism genes were present as a single
351 cluster, but the cluster differed significantly between species. In a large group of *A.*
352 *hydrophila* strains, the region contained the *iolXYZ* transporter genes and IolG clustered
353 divergently with *Pectobacterium* and *Dickeya* species. An *iol* cluster containing a Sodium
354 Solute Symporter (SSS) type transporter was present in all other *Aeromonas* species
355 examined and in these species was only present in a few to one isolate of each species.

356 In *A. hydrophila* strains, the cluster was inserted adjacent to a tRNA-Leu locus and
357 clustered with integrase and phage genes, markers of horizontal gene transfer. In *A.*
358 *dhakensis* strains, also an important pathogen of fish, insertion occurred at the tRNA-Ser
359 locus, a 27 gene region with homology to phage genes and a restriction modification
360 system was present followed by the *iol* gene cluster. In *A. media, A. allosaccharophila,* and
361 *A. finlandersis,* the *iol* gene cluster was also present adjacent to a tRNA-Ser locus but had
362 different flanking genes and was only present in one strain of these species.

363 **Discussion**

364 Our examination of *V. coralliilyticus* response to changes in osmotic stress under
365 different growth temperatures demonstrated the importance of NaCl for optimal
366 growth and growth at high temperatures. We have shown that *V. coralliilyticus* can
367 grow in 1% - 4% NaCl but grows optimal in 2% NaCl at 28°C and has an absolute
368 requirement for NaCl for growth at 37°C. Compared to other *Vibrio* species that grow in
369 up to 7% NaCl without the addition of compatible solutes, *V. coralliilyticus* has a
370 relatively low salinity tolerance of 4% NaCl. A major difference between *V. coralliilyticus*
371 and these *Vibrio* species is the absence of the ectoine biosynthesis cluster *ectABC*, which
372 is required for biosynthesis of ectoine *de novo*. However, similar to other *Vibrio* species,
373 *V. coralliilyticus* could uptake a wide range of compatible solutes from their surrounding
374 environment such choline, GB, DMSP, DMG, and ectoine for osmotic protection. *Myo*-
375 inositol is a compatible solute more commonly associated with a few hyperthermophile
376 bacteria as well as many eukaryotic species such as algae and plants (90-93). Therefore,
377 it came as no surprise that *V. coralliilyticus* did not use *myo*-inositol for osmotic
378 protection. However, our bioinformatics analysis did identify a genomic region on
379 chromosome 2 that contained *myo*-inositol metabolic gene clusters present in all *V.*
380 *coralliilyticus* isolates. We showed *V. coralliilyticus* can utilize *myo*-inositol as a sole
381 carbon source with a 3 h lag phase. This is significant since previous studies on the

382 Gram-negative human pathogens such as *Salmonella enterica* have shown a lag time of
383 over 40 hours (69, 71, 72, 75). The Gram-negative soil bacteria *Caulobacter vibrioides*
384 (formerly *crescentus*) (70, 81), *Rhizobium leguminosarum* (formerly *trifolii*) (76), and
385 *Sinorhizobium meliloti* (94) were also shown to have a long lag times of about 14 h when
386 grown on *myo*-inositol as a sole carbon source (81). A possible reason for this efficient
387 use of *myo*-inositol in *V. coralliilyticus* is the presence of two transporters for uptake into
388 the cell, an MFS-type IolT and an ABC-type family transporter IolXYZ. As shown in the
389 deletion mutant analysis of these systems, both have somewhat similar *myo*-inositol
390 uptake affinities. Alternatively, the regulation of the catabolism genes may be different
391 in these species.

392 Examination of the evolutionary history of the proteins IolG and IolA among
393 *Vibrionaceae* demonstrated that the two regions were acquired separately in many
394 species indicating convergent evolution of this phenotypic trait. The closest relative to
395 IolG outside of the Vibrionales were members of the Enterobacterales (*Dickeya,*
396 *Pectobacterium*) and Aeromonadales (*Aeromonas*). In all fifteen *Pectobacterium* species, the
397 genes are present within a highly homologous single cluster indicating it was acquired
398 once within the genus (**Fig. 10**). In the ten *Dickeya* species examined a similar gene
399 cluster as found in *Pectobacterium* was present with the addition of 3 genes inserted
400 between *iolD* and *iolG* (**Fig. 10**). Two different *myo*-inositol clusters were present in
401 *Aeromonas* species. In the hypervirulent *A. hydrophila* species associated with epidemic
402 disease in fish aquaculture farms in China and the USA, the single *iol* cluster contained
403 the IolXYZ ABC-type transporter and was inserted at a tRNA-Leu locus. This insertion
404 was within a region that contained an integrase and phage genes on one flank and an
405 IS3 element on the opposite flank. Previous studies have showed that hypervirulent *A.*
406 *hydrophila* strains all contained an *iol* cluster and could utilize *myo*-inositol as a sole
407 carbon source. This is an important trait differentiating these strains from other *A.*

408 *hydrophila* isolates (95-97). In *A. hydrophila* strains WCX23 and 23-C-23, the *iol* metabolic
409 gene cluster was inserted next to a tRNA-His locus, contained a sodium solute
410 symporter (SSS) and was flanked on both side by genes encoding a type six secretion
411 system (T6SS). Overall, the data suggest that in *Aeromonas,* the *iol* gene cluster is likely a
412 recent addition acquired on a mobile genetic element. This contrasts with what we
413 observed in *Vibrio* species.

414 Heightened ocean temperatures have resulted in increased *Vibrio* species abundance
415 worldwide (4, 29, 98-101). The increased abundance of *V. coralliilyticus* during ocean
416 warming has also been documented and believed to be a major contributing factor to
417 coral bleaching(2). We hypothesize that this increased abundance could contribute to a
418 breakdown in the coral-algae symbiosis. Perhaps *V. coralliilyticus* consumption of *myo*-
419 inositol is depleting the availability of *myo*-inositol as a stress protectant for algae,
420 which could then lead to a decline in algal abundance. In addition, *myo*-inositol is used
421 as a building block in various signal transduction pathways, and the ability of *V.*
422 *coralliilyticus* to catabolize this sugar poses a means for signaling interference. Both
423 potentially contributing to increased *myo*-inositol consumption and an inhibition of
424 algal survival eventually leading to coral bleaching. Alternatively, the consumption of
425 *myo*-inositol by *V. coralliilyticus* may be a fitness factor that gives it a competitive
426 advantage over members of the coral microbiome.

427 **Materials and Methods**

428 **Bacterial strains, media, and culture conditions**. All strains and plasmids used in this
429 study are listed in **Table 2**. *Vibrio coralliilyticus* strain CN52H-1 (7) was used in this
430 study. Unless stated otherwise, *V. coralliilyticus* was grown at 28°C in either lysogeny
431 broth (LB) (Fisher Scientific, Fair Lawn, NJ) with 2% (wt/vol) NaCl (LB 2%NaCl) or M9
432 minimal media (47.8 mM Na_2HPO_4, 22 mM KH_2PO_4, 18.7 mM NH_4Cl, 8.6 mM NaCl;
433 Sigma Aldrich) supplemented with 2 mM $MgSO_4$, 0.1 mM $CaCl_2$, 2% (wt/vol) NaCl and

434 20 mM glucose as the sole carbon source (M9G 2% NaCl). *Escherichia coli* strains were
435 grown in LB supplemented with 1% (wt/vol) NaCl (LB1%) at 37°C. The strain *E. coli*
436 β2155 *λpir* is a diaminopimelic acid (DAP) auxotroph and was grown supplemented
437 with 0.3 mM DAP (102). The *V. harveyi* strain used for analysis was strain 393 (103).
438 Chloramphenicol (Cm) was added to media at a concentration of 12.5 μg/mL when
439 specified.

440 **Osmotic Stress Growth Analysis**. *Vibrio coralliilyticus* was grown overnight in M9G 1%
441 NaCl at 28°C with aeration. A 2% inoculation of the overnight culture into fresh M9G
442 1% NaCl was grown to OD ~ 0.50 at 28°C with aeration. Exponential cultures were
443 inoculated 1:40 into 200 μL fresh M9G media containing 1% to 6% NaCl. When using
444 compatible solutes glycine betaine (GB), dimethylsulfoniopropionate (DMSP), ectoine,
445 choline, dimethylglycine (DMG), trimethylamine N-oxide (TMAO), gamma-
446 aminobutyric acid (GABA), creatine, *myo*-inositol (MI), and glycerol were used at a final
447 concentration of 1 mM in M9G 5% NaCl. Plates were incubated at 28°C with
448 intermittent shaking for 1 min every hour. Optical densities were taken at 595 nm every
449 hour for a total of 24 h using a Tecan Sunrise microplate reader and Magellan plate
450 reader software (Tecan Systems Inc., San Jose, CA).

451 **Deletion Mutant Construction**. In-frame nonpolar deletion mutants of *iolG*
452 (HRJ43_RS06535), *iolT1* (HRJ43_RS06585), and *iolX* (HRJ43_RS06670) were constructed
453 using SOE PCR and allelic exchange as previously described (104). Truncations of the
454 genes of interest, *iolG* (18-bp of the 984-bp gene), *iolT1* (30-bp of the 1452-bp gene), and
455 *iolX* (24-bp of the 1008-bp) were generated using the primers listed in **Table 3**. The
456 truncated gene products were ligated with the suicide vector pDS132 using the Gibson
457 assembly protocol and then transformed into *E. coli* Dh5α λpir (105, 106). The plasmids
458 pDSΔ*iolG*, pDSΔ*iolT1,* and pDSΔ*iolX* were then purified and transformed into *E. coli*
459 β2155 *λpir* (DAP auxotroph). Then conjugation followed by homologous recombination

460 into the *V. coralliilyticus* CN52H-1 genome was completed. To select for the single
461 crossover of the plasmids into the genome, plating onto chloramphenicol (Cm) was
462 used and colonies were screened via PCR for the truncated allele. To induce a double-
463 crossover event, the single-cross strains were grown overnight in the absence of Cm.
464 The cultures were then spread on 10% sucrose plates, and healthy colonies were
465 screened for gene truncation, and plasmid excision. Colonies that still contained the
466 plasmid would appear soupy on the 10% sucrose plates because of the presence of *sacB*
467 selectable marker. In-frame deletions were confirmed with sequencing.

468 **Metabolic Growth Analysis**. Strains were grown overnight in M9G 2% NaCl at 28°C
469 with aeration. Overnight cultures were washed twice with PBS and then inoculated 1:40
470 into 200 μL fresh M9 media supplemented with 2% NaCl, and specified carbon source
471 (glucose (20 mM) or *myo*-inositol (20 mM)). Plates were incubated at 28°C with
472 intermittent shaking for 1 min during every hour. Optical densities were taken at 595
473 nm every hour for a total of 30 h using a Tecan Sunrise microplate reader and Magellan
474 plate reader software (Tecan Systems Inc., San Jose, CA).

475 **Preparation of cellular extracts and proton nuclear magnetic resonance (^{1}H-NMR)**.
476 Wild type *V. coralliilyticus* was grown overnight at 28°C in M9G 4% NaCl supplemented
477 with 1 mM choline. Stationary phase cells were then pelleted and washed twice with
478 PBS. Three freeze-thaw cycles were performed with the cell pellets to increase lysis, and
479 the cells were then resuspended in 750 μL ethanol. Debris was pelleted by
480 centrifugation, and the ethanol solution was transferred to a clean tube and evaporated
481 under vacuum. Then deuterium oxide (D_2O) was used to resuspend the pellet, and
482 insoluble material was removed by centrifugation. The solution was then transferred to
483 a 5-mm NMR tube for analysis on a Bruker AVANCE 600NMR spectrometer at a proton
484 frequency of 600.13 MHz with a sweep of 12,376 Hz and a relaxation delay of 5 s.
485 Sixteen scans were co-added for each spectrum.

486 **Phylogenetic analysis**. Phylogenetic analysis was conducted using the program MEGA
487 X (107). The evolutionary history of IolG, IolA and RpoB was inferred using the
488 Neighbor-Joining method (108). The evolutionary distances were computed using the
489 JTT matrix-based method and are in the units of the number of amino acid substitutions
490 per site (109). The rate variation among sites was modeled with a gamma distribution
491 (shape parameter = 5). All ambiguous positions were removed for each sequence pair
492 (pairwise deletion option).

493 **Ligand Docking Modeling**. The transporter amino acid sequences were downloaded
494 from NCBI and aligned using ClustalW(89): *B. subtilis* IolT (WP_003234027.1), *S. enterica*
495 IolT1 (NP_463279.1), *V. coralliilyticus* IolT1 (WP_099607352.1), *V. coralliilyticus* IolT2
496 (WP_172853823.1), *C. crescentus* IbpA (WP_010918744.1), and *V. coralliilyticus* IolX
497 (WP_227495657.1). Transporter alignments were displayed and annotated using ESPript
498 (http://espript.ibcp.fr/ESPript/cgi-bin/ESPript.cgi) (110). Obtained predicted protein
499 structures from AlphaFold (111). The Ligand model for *myo*-inositol (MI) was obtained
500 from Chemical Entities of Biological Interest (CheBI) EMBL (112). Polar hydrogens were
501 added to the ligand structures. The docking experiments were performed using
502 SeamDock which was set to use docking parameters for the Vina software (Spacing: 1.0,
503 Mode: 2, Energy Range: 5, Exhaustiveness: 8) (113).

504

505

506

507

508

509

510 **Figure Legends**

511 **Fig. 1. Pathway of m*yo*-inositol catabolism.** The pathway presented is based upon
512 enzymological studies in *B. subtilis* and genome comparison. The proteins and
513 intermediate compounds in the pathway are displayed.

514 **Fig. 2. *Vibrio coralliilyticus* NaCl tolerance range.** Growth curve analysis of *V.*
515 *coralliilyticus* CN52H-1 in minimal media with glucose (M9G) containing 1% to 5%
516 NaCl. Growth was measured every hour for 24 h at 28°C. Mean and standard deviation
517 of two biological replicates are shown.

518 **Fig. 3. *V. coralliilyticus* compatible solute biosynthesis and uptake systems. A.**
519 Predicted genes for glycine betaine biosynthesis and compatible solute transporters in
520 *V. coralliilyticus* **B. Glycine betaine biosynthesis from choline.** H-NMR spectra of *V.*
521 *coralliilyticus* CN52H-1 cellular extract grown in minimal media (M9G) with 4% NaCl
522 with the addition of 1mM choline. The spectra peaks corresponding to glycine betaine
523 are labeled (2 and 3) and the chemical structure is provided.

524 **Fig. 4. High variability in chromosomal organization of *iol* genes among bacteria.**
525 Schematic of the gene order of myo-inositol transporter, catabolism and regulatory
526 genes among previously characterized species and *Vibrio*. Arrows represent open
527 reading frames and direction of arrow represents direct of transcription. Arrows of
528 similar color represent similar proteins/genes.

529 **Fig. 5. *V. coralliilyticus* utilized *myo*-inositol as a sole carbon source.** Growth curve
530 analysis in minimal media (M9) containing either 20 mM Glucose (black squares) or
531 20mM *myo*-inositol (blue triangles). **A.** *V. coralliilyticus* CN52H-1. **B.** *V. harveyi* 393 **C.** *V.*
532 *coralliilyticus* Δ*iolG.* Growth was measured every hour for 30 h at 28°C. Mean and
533 standard deviation of two biological replicates are shown.

534 **Fig. 6. Favorable *myo*-inositol ligand docking predicted for *V. coralliilyticus***
535 **transporters.** Results of *myo*-inositol docking study showing putative residues
536 mediating the interactions with the ligand. Residues that are predicted to interact with
537 *myo*-inositol are shown with an up arrow. **A.** MFS-type transporters; *V. coralliilyticus*
538 IolT1 (WP_099607352.1, blue arrows), *V. coralliilyticus* IolT2 (WP_172853823.1), *B. subtilis*
539 IolT (WP_003234027.1, orange arrows), *S. enterica* IolT1 (NP_463279.1, green arrows).
540 Both *B. subtilis* IolT and *S. enterica* IolT1 take up *myo*-inositol. **B.** ABC-type transporter
541 substrate binding proteins; *V. coralliilyticus* IolX (WP_227495657.1, blue arrows) and *C.*
542 *vibrioides* IbpA (WP_010918744.1, green arrows). *C. vibrioides* has been shown to uptake
543 *myo*-inositol using this ABC-type transporter.

544 **Fig. 7. Identification of *myo*-inositol transporters in *V. coralliilyticus*.** Growth analysis
545 of wild type, Δ*iolT1*, Δ*iolX*, and Δ*iolT1*/ Δ*iolX* in minimal media (M9G) with 20 mM *myo*-
546 inositol as a sole carbon source. Growth was measured every hour for 30 h at 28°C.
547 Mean and standard deviation of two biological replicates are shown.

548 **Fig. 8. Phylogenetic distribution of IolG and Iol cluster organization among**
549 ***Vibrionaceae*. A.** IolG evolutionary history was inferred using the Neighbor-Joining
550 method (108) with bootstrap value of 1000 (114). The optimal tree with the sum of
551 branch length = 4.11930205 is shown. The tree is drawn to scale, and evolutionary
552 distances were computed using the JTT matrix-based method (109) with units of the
553 number of amino acid substitutions per site. Shown are 53 amino acid sequences,
554 ambiguous positions were removed for each sequence pair (pairwise deletion option)
555 with a total of 332 positions. Evolutionary analyses were conducted in MEGA X (107).
556 Adjacent to the tree are gene order diagrams representative of the designated species. **B**.
557 Iol cluster organization among *Vibrionaceae* species. Arrows represent open rreading
558 frame and direction of transcription.

559 **Fig. 9. Phylogenetic distribution of IolA and the housekeeping protein RpoB. A.** IolA
560 evolutionary history was inferred using the Neighbor-Joining method (108) with
561 bootstrap value of 1000 (114). The optimal tree with the sum of branch length =
562 2.37747408 is shown. The tree is drawn to scale, and evolutionary distances were
563 computed using the JTT matrix-based method (109) with units of the number of amino
564 acid substitutions per site. Shown are 43 amino acid sequences, ambiguous positions
565 were removed for each sequence pair (pairwise deletion option) with a total of 510
566 positions. Evolutionary analyses were conducted in MEGA X (107). **B**. Housekeeping
567 protein RpoB phylogeny based on the same set of species that contained IolG
568 constructed using the Neighbor-Joining method.

569 **Fig. 10. IolG from *Vibrio* clustered with members of *Aeromonas*, *Pectobacterium*, and**
570 ***Dickeya*.** Evolutionary analyses were conducted in MEGA X (107). IolG phylogeny was
571 inferred using the Neighbor-Joining method (108) and the optimal tree with the sum of
572 branch length = 5.23592824 is shown. The percentage of replicate trees in which the
573 associated taxa clustered together in the bootstrap test (1000 replicates) are shown next
574 to the branches and distances were computed using the JTT matrix-based method and
575 are in the units of the number of amino acid substitutions per site (114). The rate
576 variation among sites was modeled with a gamma distribution (shape parameter = 5).
577 This analysis involved 81 amino acid sequences. All ambiguous positions were
578 removed for each sequence pair (pairwise deletion option). There were a total of 333
579 positions in the final dataset.

580

581 **Table 1.** Growth curve analysis of *V. coralliilyticus* in minimal media containing glucose
582 (M9G) and 5% NaCl supplemented with 1mM of GB (glycine betaine), DMSP
583 (dimethylsulfoniopropionate), Ectoine, Choline, MI (*myo*-inositol), DMG
584 (dimethylglycine), trimethylamine N-oxide (TMAO), gamma-aminobutyric acid
585 (GABA), Creatine, or Glycerol. Growth was measured every hour for 24 h at 28°C.
586 Maximum growth rate, Area under the curve, and final OD presented here for two
587 biological replicates.

588

M9G + 5% NaCl	**Max. Growth Rate (h^{-1})**	**Area Under Curve**	**Final OD**
No CS	0	0	0
GB	0.56	6.1	0.55
DMSP	0.55	6.3	0.67
Ectoine	0.48	3.9	0.69
Choline	0.48	1.9	0.45
***myo*-inositol**	0	0	0
DMG	0.53	4.6	0.52
TMAO	0	0	0
GABA	0.31	0.9	0.23
Creatine	0.38	1.2	0.31
Glycerol	0	0	0

589

590 **Table 2. Strains and plasmids used in this study**

Strain or plasmid	Genotype or description	Reference(s) or source
Vibrio coralliilyticus		
CN52H-1	Environmental isolate from reef	Ushijima et al., 2020
Δ*iolG*	Deletion of HRJ43_RS06535 from CN52H-1	This study
Δ*iolT1*	Deletion of HRJ43_RS06585 from CN52H-1	This study
Δ*iolX*	Deletion of HRJ43_RS06670 from CN52H-1	This study
Δ*iolT1*/Δ*iolX*	*iolX* deletion in Δ*iolT2* mutant background	This study
Vibrio harveyi		
393	Isolated from barramundi in Australia	Pederson et al., 1998
Escherichia coli		
DH5α *λpir*		ThermoFisher Scientific
B2155 *λpir*	Δ*dapA*::erm pir for bacterial conjugation	(Dehio & Meyer, 1997)
Plasmids		
pDS132	Suicide plasmid; CmR; *sacB*, R6Kg ori	(Philippe et al., 2004)
pDS*iolG*	pDS132 harboring truncated *iolG* allele	This study
pDS*iolT1*	pDS132 harboring truncated *iolT1* allele	This study
pDS*iolX*	pDS132 harboring truncated *iolX* allele	This study

591

592

593

594

595

596 **Table 3. Primers used in this study**

Primer Name	Sequence (5′ – 3′)	Length (bp)
Mutant Primers		
AB fwd_*iolG*	accgcatgcgatatcgagctGTGGTTGAGGTGTACACC	549
AB rev_*iolG*	cttatagtgaATTAAACATTCTGTACTCCTTACAG	
CD fwd_*iolG*	aatgtttaatTCACTATAAGAAATTCAACCGGAAG	549
CD rev_*iolG*	gtggaattcccgggagagctTCCGGAAATCGTCCGCTATTTC	
flank fwd_*iolG*	acatcggtcagcgtatgtct	2369
flank rev_*iolG*	aaccgcgactacctttacca	
AB fwd_*iolT1*	accgcatgcgatatcgagctATGCTTTTCATCTCTCGTTC	549
AB rev_*iolT1*	gtacgtgcgcATGACTCGATGACATGTTTC	
CD fwd_*iolT1*	atcgagtcatGCGCACGTACAATAACATTG	549
CD rev_*iolT1*	gtggaattcccgggagagctCGATACCCCTGAAATGAGG	
flank fwd_*iolT1*	actttgttcccagctccgta	2809
flank rev_*iolT1*	gcgaacaaacaatggtgctg	
AB fwd_*iolX*	accgcatgcgatatcgagctCAACTATCGCCGAATAAGGTTATTTG	606
AB rev_*iolX*	aacctttttgTAATGATGGCATCATTGCC	
CD fwd_*iolX*	gccatcattaCAAAAAGGTTAATGGAATAACAGC	465
CD rev_*iolX*	gtggaattcccgggagagctATCGCGATACATCTTATCGTG	
flank fwd_*iolX*	cgatgacccaccgagatact	2248
flank rev_*iolX*	caccgtcagttcagtcatcg	

597

598

599

600 **References**

601 1. Santos Ede O, Alves N, Jr., Dias GM, Mazotto AM, Vermelho A, Vora GJ, Wilson
602 B, Beltran VH, Bourne DG, Le Roux F, Thompson FL. 2011. Genomic and
603 proteomic analyses of the coral pathogen Vibrio coralliilyticus reveal a diverse
604 virulence repertoire. Isme j 5:1471-83.
605 2. Ben-Haim Y, Zicherman-Keren M, Rosenberg E. 2003. Temperature-regulated
606 bleaching and lysis of the coral Pocillopora damicornis by the novel pathogen
607 Vibrio coralliilyticus. Appl Environ Microbiol 69:4236-42.
608 3. Kooperman N, Ben-Dov E, Kramarsky-Winter E, Barak Z, Kushmaro A. 2007.
609 Coral mucus-associated bacterial communities from natural and aquarium
610 environments. FEMS Microbiol Lett 276:106-13.
611 4. Kimes NE, Grim CJ, Johnson WR, Hasan NA, Tall BD, Kothary MH, Kiss H,
612 Munk AC, Tapia R, Green L, Detter C, Bruce DC, Brettin TS, Colwell RR, Morris
613 PJ. 2012. Temperature regulation of virulence factors in the pathogen Vibrio
614 coralliilyticus. Isme j 6:835-46.
615 5. Godwin S, Bent E, Borneman J, Pereg L. 2012. The role of coral-associated
616 bacterial communities in Australian Subtropical White Syndrome of Turbinaria
617 mesenterina. PLoS One 7:e44243.

618 6. Ushijima B, Saw JH, Videau P, Häse CC. 2022. Comparison of Vibrio
619 coralliilyticus virulence in Pacific oyster larvae and corals. Microbiology
620 (Reading) 168(4).
621 7. Ushijima B, Meyer JL, Thompson S, Pitts K, Marusich MF, Tittl J, Weatherup E,
622 Reu J, Wetzell R, Aeby GS, Häse CC, Paul VJ. 2020. Disease Diagnostics and
623 Potential Coinfections by Vibrio coralliilyticus During an Ongoing Coral Disease
624 Outbreak in Florida. Front Microbiol 11:569354.
625 8. Vidal-Dupiol J, Ladrière O, Meistertzheim AL, Fouré L, Adjeroud M, Mitta G.
626 2011. Physiological responses of the scleractinian coral Pocillopora damicornis to
627 bacterial stress from Vibrio coralliilyticus. J Exp Biol 214:1533-45.
628 9. Ben-Haim Y, Rosenberg E. 2002. A novel Vibrio sp. pathogen of the coral
629 Pocillopora damicornis. Marine Biology 141:47-55.
630 10. Rosenberg E, Ben-Haim Y. 2002. Microbial diseases of corals and global
631 warming. Environ Microbiol 4:318-26.
632 11. Ben-Haim Y, Thompson FL, Thompson CC, Cnockaert MC, Hoste B, Swings J,
633 Rosenberg E. 2003. Vibrio coralliilyticus sp. nov., a temperature-dependent
634 pathogen of the coral Pocillopora damicornis. Int J Syst Evol Microbiol 53:309-
635 315.
636 12. Bourne DG, Munn CB. 2005. Diversity of bacteria associated with the coral
637 Pocillopora damicornis from the Great Barrier Reef. Environ Microbiol 7:1162-74.

638 13. Sussman M, Willis BL, Victor S, Bourne DG. 2008. Coral pathogens identified for
639 White Syndrome (WS) epizootics in the Indo-Pacific. PLoS One 3:e2393.
640 14. Munn CB. 2015. The Role of Vibrios in Diseases of Corals. Microbiol Spectr 3(4).
641 15. Ushijima B, Videau P, Burger AH, Shore-Maggio A, Runyon CM, Sudek M, Aeby
642 GS, Callahan SM. 2014. Vibrio coralliilyticus strain OCN008 is an etiological
643 agent of acute Montipora white syndrome. Appl Environ Microbiol 80:2102-9.
644 16. Ushijima B, Videau P, Poscablo D, Stengel JW, Beurmann S, Burger AH, Aeby
645 GS, Callahan SM. 2016. Mutation of the toxR or mshA genes from Vibrio
646 coralliilyticus strain OCN014 reduces infection of the coral Acropora cytherea.
647 Environ Microbiol 18:4055-4067.
648 17. Richards GP, Watson MA, Needleman DS, Church KM, Häse CC. 2015.
649 Mortalities of Eastern and Pacific oyster Larvae caused by the pathogens Vibrio
650 coralliilyticus and Vibrio tubiashii. Appl Environ Microbiol 81:292-7.
651 18. Ushijima B, Richards GP, Watson MA, Schubiger CB, Häse CC. 2018. Factors
652 affecting infection of corals and larval oysters by Vibrio coralliilyticus. PLoS One
653 13:e0199475.
654 19. Richards GP, Watson MA, Madison D, Soffer N, Needleman DS, Soroka DS,
655 Uknalis J, Baranzoni GM, Church KM, Polson SW, Elston R, Langdon C,
656 Sulakvelidze A. 2021. Bacteriophages against Vibrio coralliilyticus and Vibrio

657 tubiashii: Isolation, Characterization, and Remediation of Larval Oyster
658 Mortalities. Appl Environ Microbiol 87(10):e00008-21.
659 20. Kim HJ, Giri SS, Kim SG, Kim SW, Kwon J, Lee SB, Park SC. 2020. Isolation and
660 Characterization of Two Bacteriophages and Their Preventive Effects against
661 Pathogenic Vibrio coralliilyticus Causing Mortality of Pacific Oyster (Crassostrea
662 gigas) Larvae. Microorganisms 8(6):926.
663 21. Kim HJ, Jun JW, Giri SS, Chi C, Yun S, Kim SG, Kim SW, Han SJ, Kwon J, Oh
664 WT, Lee SB, Kim JH, Park SC. 2020. Identification and Genome Analysis of
665 Vibrio coralliilyticus Causing Mortality of Pacific Oyster (Crassostrea gigas)
666 Larvae. Pathogens 9(3):206.
667 22. Richards GP, Kingham BF, Shevchenko O, Watson MA, Needleman DS. 2018.
668 Complete Genome Sequence of Vibrio coralliilyticus RE22, a Marine Bacterium
669 Pathogenic toward Larval Shellfish. Microbiol Resour Announc 7(17):e01332-18.
670 23. Arboleda M, Reichardt W. 2009. Epizoic communities of prokaryotes on healthy
671 and diseased scleractinian corals in Lingayen Gulf, Philippines. Microb Ecol
672 57:117-28.
673 24. Koenig JE, Bourne DG, Curtis B, Dlutek M, Stokes HW, Doolittle WF, Boucher Y.
674 2011. Coral-mucus-associated Vibrio integrons in the Great Barrier Reef: genomic
675 hotspots for environmental adaptation. Isme j 5:962-72.

676 25. Kvennefors EC, Sampayo E, Ridgway T, Barnes AC, Hoegh-Guldberg O. 2010.
677 Bacterial communities of two ubiquitous Great Barrier Reef corals reveals both
678 site- and species-specificity of common bacterial associates. PLoS One 5:e10401.
679 26. Gibbin E, Gavish A, Krueger T, Kramarsky-Winter E, Shapiro O, Guiet R, Jensen
680 L, Vardi A, Meibom A. 2019. Vibrio coralliilyticus infection triggers a
681 behavioural response and perturbs nutritional exchange and tissue integrity in a
682 symbiotic coral. Isme j 13:989-1003.
683 27. Vega Thurber R, Willner-Hall D, Rodriguez-Mueller B, Desnues C, Edwards RA,
684 Angly F, Dinsdale E, Kelly L, Rohwer F. 2009. Metagenomic analysis of stressed
685 coral holobionts. Environ Microbiol 11:2148-63.
686 28. Tout J, Siboni N, Messer LF, Garren M, Stocker R, Webster NS, Ralph PJ,
687 Seymour JR. 2015. Increased seawater temperature increases the abundance and
688 alters the structure of natural Vibrio populations associated with the coral
689 Pocillopora damicornis. Front Microbiol 6:432.
690 29. Vezzulli L, Previati M, Pruzzo C, Marchese A, Bourne DG, Cerrano C. 2010.
691 Vibrio infections triggering mass mortality events in a warming Mediterranean
692 Sea. Environ Microbiol 12:2007-19.
693 30. Garren M, Son K, Raina JB, Rusconi R, Menolascina F, Shapiro OH, Tout J,
694 Bourne DG, Seymour JR, Stocker R. 2014. A bacterial pathogen uses

695 dimethylsulfoniopropionate as a cue to target heat-stressed corals. Isme j 8:999-
696 1007.
697 31. Vidal-Dupiol J, Dheilly NM, Rondon R, Grunau C, Cosseau C, Smith KM, Freitag
698 M, Adjeroud M, Mitta G. 2014. Thermal stress triggers broad Pocillopora
699 damicornis transcriptomic remodeling, while Vibrio coralliilyticus infection
700 induces a more targeted immuno-suppression response. PLoS One 9:e107672.
701 32. Garren M, Son K, Tout J, Seymour JR, Stocker R. 2016. Temperature-induced
702 behavioral switches in a bacterial coral pathogen. Isme j 10:1363-72.
703 33. Wu Y, Zhou Z, Wang J, Luo J, Wang L, Zhang Y. 2019. Temperature regulates the
704 recognition activities of a galectin to pathogen and symbiont in the scleractinian
705 coral Pocillopora damicornis. Dev Comp Immunol 96:103-110.
706 34. Zhou Z, Zhao S, Tang J, Liu Z, Wu Y, Wang Y, Lin S. 2019. Altered Immune
707 Landscape and Disrupted Coral-Symbiodinium Symbiosis in the Scleractinian
708 Coral Pocillopora damicornis by Vibrio coralliilyticus Challenge. Front Physiol
709 10:366.
710 35. Rosenberg E, Kushmaro A, Kramarsky-Winter E, Banin E, Yossi L. 2009. The role
711 of microorganisms in coral bleaching. Isme j 3:139-46.
712 36. Roth MS. 2014. The engine of the reef: photobiology of the coral-algal symbiosis.
713 Front Microbiol 5:422.

714 37. Kopp C, Domart-Coulon I, Escrig S, Humbel BM, Hignette M, Meibom A. 2015.
715 Subcellular investigation of photosynthesis-driven carbon assimilation in the
716 symbiotic reef coral Pocillopora damicornis. mBio 6(1):e02299-14.
717 38. Sproles AE, Kirk NL, Kitchen SA, Oakley CA, Grossman AR, Weis VM, Davy SK.
718 2018. Phylogenetic characterization of transporter proteins in the cnidarian-
719 dinoflagellate symbiosis. Mol Phylogenet Evol 120:307-320.
720 39. Matthews JL, Oakley CA, Lutz A, Hillyer KE, Roessner U, Grossman AR, Weis
721 VM, Davy SK. 2018. Partner switching and metabolic flux in a model cnidarian-
722 dinoflagellate symbiosis. Proc Biol Sci 285(1892):20182336.
723 40. LaJeunesse TC, Thornhill DJ, Cox EF, Stanton FG, Fitt WK, Schmidt GW. 2004.
724 High diversity and host specificity observed among symbiotic dinoflagellates in
725 reef coral communities from Hawaii. Coral Reefs 23:596-603.
726 41. Tanaka Y, Miyajima T, Koike I, Hayashibara T, Ogawa H. 2006. Translocation
727 and conservation of organic nitrogen within the coral-zooxanthella symbiotic
728 system of Acropora pulchra, as demonstrated by dual isotope-labeling
729 techniques. Journal of Experimental Marine Biology and Ecology 336:110-119.
730 42. Rädecker N, Pogoreutz C, Voolstra CR, Wiedenmann J, Wild C. 2015. Nitrogen
731 cycling in corals: the key to understanding holobiont functioning? Trends
732 Microbiol 23:490-7.

733 43. Rosic N, Ling EY, Chan CK, Lee HC, Kaniewska P, Edwards D, Dove S, Hoegh-
734 Guldberg O. 2015. Unfolding the secrets of coral-algal symbiosis. Isme j 9:844-56.
735 44. Cui G, Liew YJ, Konciute MK, Zhan Y, Hung SH, Thistle J, Gastoldi L, Schmidt-
736 Roach S, Dekker J, Aranda M. 2022. Nutritional control regulates symbiont
737 proliferation and life history in coral-dinoflagellate symbiosis. BMC Biol 20:103.
738 45. Rands ML, Loughman BC, Douglas AE. 1993. The Symbiotic Interface in an Alga-
739 Invertebrate Symbiosis. Proceedings: Biological Sciences 253:161-165.
740 46. Muscatine L, Porter JW. 1977. Reef Corals: Mutualistic Symbioses Adapted to
741 Nutrient-Poor Environments. BioScience 27:454-460.
742 47. Aranda M, Li Y, Liew YJ, Baumgarten S, Simakov O, Wilson MC, Piel J, Ashoor
743 H, Bougouffa S, Bajic VB, Ryu T, Ravasi T, Bayer T, Micklem G, Kim H, Bhak J,
744 LaJeunesse TC, Voolstra CR. 2016. Genomes of coral dinoflagellate symbionts
745 highlight evolutionary adaptations conducive to a symbiotic lifestyle. Sci Rep
746 6:39734.
747 48. LaJeunesse TC, Parkinson JE, Gabrielson PW, Jeong HJ, Reimer JD, Voolstra CR,
748 Santos SR. 2018. Systematic Revision of Symbiodiniaceae Highlights the
749 Antiquity and Diversity of Coral Endosymbionts. Curr Biol 28:2570-2580.e6.
750 49. Ashley IA, Kitchen SA, Gorman LM, Grossman AR, Oakley CA, Suggett DJ, Weis
751 VM, Rosset SL, Davy SK. 2022. Genomic conservation and putative downstream

752 functionality of the phosphatidylinositol signalling pathway in the cnidarian-
753 dinoflagellate symbiosis. Front Microbiol 13:1094255.
754 50. Lohia A, Hait NC, Majumder AL. 1999. L-myo-Inositol 1-phosphate synthase
755 from Entamoeba histolytica. Mol Biochem Parasitol 98:67-79.
756 51. Nikitashina V, Stettin D, Pohnert G. 2022. Metabolic adaptation of diatoms to
757 hypersalinity. Phytochemistry 201:113267.
758 52. Lehnert EM, Mouchka ME, Burriesci MS, Gallo ND, Schwarz JA, Pringle JR. 2014.
759 Extensive differences in gene expression between symbiotic and aposymbiotic
760 cnidarians. G3 (Bethesda) 4:277-95.
761 53. Michell RH. 2008. Inositol derivatives: evolution and functions. Nat Rev Mol Cell
762 Biol 9:151-61.
763 54. Majumder AL, Chatterjee A, Ghosh Dastidar K, Majee M. 2003. Diversification
764 and evolution of L-myo-inositol 1-phosphate synthase. FEBS Lett 553:3-10.
765 55. Turner BL, Papházy MJ, Haygarth PM, McKelvie ID. 2002. Inositol phosphates in
766 the environment. Philos Trans R Soc Lond B Biol Sci 357:449-69.
767 56. Al-Mushhin AAM, Qari SH, Fakhr MA, Alnusairi GSH, Alnusaire TS, AA AL,
768 Latef A, Ali OM, Khan AA, Soliman MH. 2021. Exogenous Myo-Inositol
769 Alleviates Salt Stress by Enhancing Antioxidants and Membrane Stability via the
770 Upregulation of Stress Responsive Genes in Chenopodium quinoa L. Plants
771 (Basel) 10(11):2416.

772 57. Das-Chatterjee A, Goswami L, Maitra S, Dastidar KG, Ray S, Majumder AL.
773 2006. Introgression of a novel salt-tolerant L-myo-inositol 1-phosphate synthase
774 from Porteresia coarctata (Roxb.) Tateoka (PcINO1) confers salt tolerance to
775 evolutionary diverse organisms. FEBS Lett 580:3980-8.
776 58. Nelson DE, Koukoumanos M, Bohnert HJ. 1999. Myo-inositol-dependent sodium
777 uptake in ice plant. Plant Physiol 119:165-72.
778 59. Blatt MR, Thiel G, Trentham DR. 1990. Reversible inactivation of K+ channels of
779 Vicia stomatal guard cells following the photolysis of caged inositol 1,4,5-
780 trisphosphate. Nature 346:766-9.
781 60. Thiel G, MacRobbie EA, Hanke DE. 1990. Raising the intracellular level of
782 inositol 1,4,5-trisphosphate changes plasma membrane ion transport in
783 characean algae. Embo j 9:1737-41.
784 61. Gillaspy GE. 2011. The cellular language of myo-inositol signaling. New Phytol
785 192:823-839.
786 62. Weber M, Fuchs TM. 2022. Metabolism in the Niche: a Large-Scale Genome-
787 Based Survey Reveals Inositol Utilization To Be Widespread among Soil,
788 Commensal, and Pathogenic Bacteria. Microbiol Spectr 10:e0201322.
789 63. Felsl A, Brokatzky D, Kröger C, Heermann R, Fuchs TM. 2023. Hierarchic
790 regulation of a metabolic pathway: H-NS, CRP, and SsrB control myo-inositol
791 utilization by Salmonella enterica. Microbiol Spectr:e0272423.

792 64. Yoshida KI, Aoyama D, Ishio I, Shibayama T, Fujita Y. 1997. Organization and
793 transcription of the myo-inositol operon, iol, of Bacillus subtilis. J Bacteriol
794 179:4591-8.
795 65. Yoshida K, Yamamoto Y, Omae K, Yamamoto M, Fujita Y. 2002. Identification of
796 two myo-inositol transporter genes of Bacillus subtilis. J Bacteriol 184:983-91.
797 66. Yoshida K, Yamaguchi M, Morinaga T, Kinehara M, Ikeuchi M, Ashida H, Fujita
798 Y. 2008. myo-Inositol catabolism in Bacillus subtilis. J Biol Chem 283:10415-24.
799 67. Yoshida KI, Sanbongi A, Murakami A, Suzuki H, Takenaka S, Takami H. 2012.
800 Three inositol dehydrogenases involved in utilization and interconversion of
801 inositol stereoisomers in a thermophile, Geobacillus kaustophilus HTA426.
802 Microbiology (Reading) 158:1942-1952.
803 68. Yoshida KI, Shibayama T, Aoyama D, Fujita Y. 1999. Interaction of a repressor
804 and its binding sites for regulation of the Bacillus subtilis iol divergon. J Mol Biol
805 285:917-29.
806 69. Berman T, Magasanik B. 1966. The pathway of myo-inositol degradation in
807 Aerobacter aerogenes. Ring scission. J Biol Chem 241:807-13.
808 70. Boutte CC, Srinivasan BS, Flannick JA, Novak AF, Martens AT, Batzoglou S,
809 Viollier PH, Crosson S. 2008. Genetic and computational identification of a
810 conserved bacterial metabolic module. PLoS Genet 4:e1000310.

811 71. Kröger C, Fuchs TM. 2009. Characterization of the myo-inositol utilization island
812 of Salmonella enterica serovar Typhimurium. J Bacteriol 191:545-54.
813 72. Kröger C, Stolz J, Fuchs TM. 2010. myo-Inositol transport by Salmonella enterica
814 serovar Typhimurium. Microbiology (Reading) 156:128-138.
815 73. Fry J, Wood M, Poole PS. 2001. Investigation of myo-inositol catabolism in
816 Rhizobium leguminosarum bv. viciae and its effect on nodulation
817 competitiveness. Mol Plant Microbe Interact 14:1016-25.
818 74. Gauchat-Feiss D, Frey J, Belet M, Deshusses J. 1985. Cloning of genes involved in
819 myo-inositol transport in a Pseudomonas sp. J Bacteriol 162:324-7.
820 75. Legakis NJ, Papavassiliou JT, Xilinas ME. 1976. Inositol as a selective substrate
821 for the growth of Klebsiellae and Serratiae. Zentralbl Bakteriol Orig A 235:453-8.
822 76. Primrose SB, Ronson CW. 1980. Polyol metabolism by Rhizobium trifolii. J
823 Bacteriol 141:1109-14.
824 77. Reber G, Belet M, Deshusses J. 1980. Energetics of myo-inositol transport in
825 Pseudomonas putida. Experientia 36:528-9.
826 78. Krings E, Krumbach K, Bathe B, Kelle R, Wendisch VF, Sahm H, Eggeling L.
827 2006. Characterization of myo-inositol utilization by Corynebacterium
828 glutamicum: the stimulon, identification of transporters, and influence on L-
829 lysine formation. J Bacteriol 188:8054-61.

830 79. Hellinckx J, Fuchs TM. 2017. Hysteresis in myo-inositol utilization by Salmonella
831 Typhimurium. Microbiologyopen 6(2):e00431.
832 80. Müller J, Spriewald S, Stecher B, Stadler E, Fuchs TM. 2019. Evolutionary
833 Stability of Salmonella Competition with the Gut Microbiota: How the
834 Environment Fosters Heterogeneity in Exploitative and Interference
835 Competition. J Mol Biol 431:4732-4748.
836 81. Herrou J, Crosson S. 2013. myo-inositol and D-ribose ligand discrimination in an
837 ABC periplasmic binding protein. J Bacteriol 195:2379-88.
838 82. Naughton LM, Blumerman SL, Carlberg M, Boyd EF. 2009. Osmoadaptation
839 among Vibrio species and unique genomic features and physiological responses
840 of Vibrio parahaemolyticus. Appl Environ Microbiol 75:2802-10.
841 83. Ongagna-Yhombi SY, Boyd EF. 2013. Biosynthesis of the osmoprotectant ectoine,
842 but not glycine betaine, is critical for survival of osmotically stressed Vibrio
843 parahaemolyticus cells. Appl Environ Microbiol 79:5038-49.
844 84. Whitaker WB, Parent MA, Naughton LM, Richards GP, Blumerman SL, Boyd EF.
845 2010. Modulation of responses of Vibrio parahaemolyticus O3:K6 to pH and
846 temperature stresses by growth at different salt concentrations. Appl Environ
847 Microbiol 76:4720-9.
848 85. Pflughoeft KJ, Kierek K, Watnick PI. 2003. Role of ectoine in Vibrio cholerae
849 osmoadaptation. Appl Environ Microbiol 69:5919-27.

850 86. Kapfhammer D, Karatan E, Pflughoeft KJ, Watnick PI. 2005. Role for glycine
851 betaine transport in Vibrio cholerae osmoadaptation and biofilm formation
852 within microbial communities. Appl Environ Microbiol 71:3840-7.
853 87. Rao NV, Shashidhar R, Bandekar JR. 2013. Comparative analysis of induction of
854 osmotic-stress-dependent genes in Vibrio vulnificus exposed to hyper- and
855 hypo-osmotic stress. Can J Microbiol 59:333-8.
856 88. Drew D, North RA, Nagarathinam K, Tanabe M. 2021. Structures and General
857 Transport Mechanisms by the Major Facilitator Superfamily (MFS). Chem Rev
858 121:5289-5335.
859 89. Thompson JD, Higgins DG, Gibson TJ. 1994. CLUSTAL W: improving the
860 sensitivity of progressive multiple sequence alignment through sequence
861 weighting, position-specific gap penalties and weight matrix choice. Nucleic
862 Acids Res 22:4673-80.
863 90. Martins LO, Carreto LS, Da Costa MS, Santos H. 1996. New compatible solutes
864 related to Di-myo-inositol-phosphate in members of the order Thermotogales. J
865 Bacteriol 178:5644-51.
866 91. Empadinhas N, Mendes V, Simões C, Santos MS, Mingote A, Lamosa P, Santos
867 H, Costa MS. 2007. Organic solutes in Rubrobacter xylanophilus: the first
868 example of di-myo-inositol-phosphate in a thermophile. Extremophiles 11:667-
869 73.

870 92. Lamosa P, Rodrigues MV, Gonçalves LG, Carr J, Ventura R, Maycock C, Raven
871 ND, Santos H. 2013. Organic solutes in the deepest phylogenetic branches of the
872 Bacteria: identification of α(1-6)glucosyl-α(1-2)glucosylglycerate in
873 Persephonella marina. Extremophiles 17:137-46.
874 93. Rodrigues MV, Borges N, Almeida CP, Lamosa P, Santos H. 2009. A unique beta-
875 1,2-mannosyltransferase of Thermotoga maritima that uses di-myo-inositol
876 phosphate as the mannosyl acceptor. J Bacteriol 191:6105-15.
877 94. Galbraith MP, Feng SF, Borneman J, Triplett EW, de Bruijn FJ, Rossbachl S. 1998.
878 A functional myo-inositol catabolism pathway is essential for rhizopine
879 utilization by Sinorhizobium meliloti. Microbiology (Reading) 144 (Pt 10):2915-
880 2924.
881 95. Xu T, Rasmussen-Ivey CR, Moen FS, Fernández-Bravo A, Lamy B, Beaz-Hidalgo
882 R, Khan CD, Castro Escarpulli G, Yasin ISM, Figueras MJ, Azzam-Sayuti M,
883 Karim MM, Alam KMM, Le TTT, Thao NHP, Addo S, Duodu S, Ali S, Latif T,
884 Mey S, Somony T, Liles MR. 2023. A Global Survey of Hypervirulent Aeromonas
885 hydrophila (vAh) Identified vAh Strains in the Lower Mekong River Basin and
886 Diverse Opportunistic Pathogens from Farmed Fish and Other Environmental
887 Sources. Microbiol Spectr 11:e0370522.
888 96. Hossain MJ, Waldbieser GC, Sun D, Capps NK, Hemstreet WB, Carlisle K,
889 Griffin MJ, Khoo L, Goodwin AE, Sonstegard TS, Schroeder S, Hayden K,

890 Newton JC, Terhune JS, Liles MR. 2013. Implication of lateral genetic transfer in
891 the emergence of Aeromonas hydrophila isolates of epidemic outbreaks in
892 channel catfish. PLoS One 8:e80943.
893 97. Rasmussen-Ivey CR, Hossain MJ, Odom SE, Terhune JS, Hemstreet WG,
894 Shoemaker CA, Zhang D, Xu DH, Griffin MJ, Liu YJ, Figueras MJ, Santos SR,
895 Newton JC, Liles MR. 2016. Classification of a Hypervirulent Aeromonas
896 hydrophila Pathotype Responsible for Epidemic Outbreaks in Warm-Water
897 Fishes. Front Microbiol 7:1615.
898 98. Boroujerdi AF, Vizcaino MI, Meyers A, Pollock EC, Huynh SL, Schock TB, Morris
899 PJ, Bearden DW. 2009. NMR-based microbial metabolomics and the temperature-
900 dependent coral pathogen Vibrio coralliilyticus. Environ Sci Technol 43:7658-64.
901 99. Rubio-Portillo E, Gago JF, Martínez-García M, Vezzulli L, Rosselló-Móra R,
902 Antón J, Ramos-Esplá AA. 2018. Vibrio communities in scleractinian corals differ
903 according to health status and geographic location in the Mediterranean Sea. Syst
904 Appl Microbiol 41:131-138.
905 100. Vezzulli L, Brettar I, Pezzati E, Reid PC, Colwell RR, Höfle MG, Pruzzo C. 2012.
906 Long-term effects of ocean warming on the prokaryotic community: evidence
907 from the vibrios. Isme j 6:21-30.
908 101. Vezzulli L, Colwell RR, Pruzzo C. 2013. Ocean warming and spread of
909 pathogenic vibrios in the aquatic environment. Microb Ecol 65:817-25.

910 102. Dehio C, Meyer M. 1997. Maintenance of broad-host-range incompatibility group
911 P and group Q plasmids and transposition of Tn5 in Bartonella henselae
912 following conjugal plasmid transfer from Escherichia coli. J Bacteriol 179:538-40.
913 103. Pederson K, Verdonck L, Austin B, Austin D, Blanch AR, Grimont PAD, Jofre J,
914 Koblavi S, Larsen JL, Tianinen T, Vigneulle M, Swings J. 1998. Taxonomic
915 evidence that Vibrio carchariae Grimes et al. 1985 is a junior synonym of Vibrio
916 harveyi (Johnson and Shunk 1936) Baumann et al. 1981. International Journal of
917 Systematic and Evolutionary Microbiology 48:748-749.
918 104. Gregory GJ, Morreale DP, Carpenter MR, Kalburge SS, Boyd EF. 2019. Quorum
919 Sensing Regulators AphA and OpaR Control Expression of the Operon
920 Responsible for Biosynthesis of the Compatible Solute Ectoine. Appl Environ
921 Microbiol 85(22):e01543-19.
922 105. Gibson DG. 2011. Enzymatic assembly of overlapping DNA fragments. Methods
923 Enzymol 498:349-61.
924 106. Philippe N, Alcaraz JP, Coursange E, Geiselmann J, Schneider D. 2004.
925 Improvement of pCVD442, a suicide plasmid for gene allele exchange in bacteria.
926 Plasmid 51:246-55.
927 107. Kumar S, Stecher G, Li M, Knyaz C, Tamura K. 2018. MEGA X: Molecular
928 Evolutionary Genetics Analysis across Computing Platforms. Mol Biol Evol
929 35:1547-1549.

930 108. Saitou N, Nei M. 1987. The neighbor-joining method: a new method for
931 reconstructing phylogenetic trees. Mol Biol Evol 4:406-25.
932 109. Jones DT, Taylor WR, Thornton JM. 1992. The rapid generation of mutation data
933 matrices from protein sequences. Comput Appl Biosci 8:275-82.
934 110. Robert X, Gouet P. 2014. Deciphering key features in protein structures with the
935 new ENDscript server. Nucleic Acids Res 42:W320-4.
936 111. Jumper J, Evans R, Pritzel A, Green T, Figurnov M, Ronneberger O,
937 Tunyasuvunakool K, Bates R, Žídek A, Potapenko A, Bridgland A, Meyer C,
938 Kohl SAA, Ballard AJ, Cowie A, Romera-Paredes B, Nikolov S, Jain R, Adler J,
939 Back T, Petersen S, Reiman D, Clancy E, Zielinski M, Steinegger M, Pacholska M,
940 Berghammer T, Bodenstein S, Silver D, Vinyals O, Senior AW, Kavukcuoglu K,
941 Kohli P, Hassabis D. 2021. Highly accurate protein structure prediction with
942 AlphaFold. Nature 596:583-589.
943 112. Hastings J, Owen G, Dekker A, Ennis M, Kale N, Muthukrishnan V, Turner S,
944 Swainston N, Mendes P, Steinbeck C. 2016. ChEBI in 2016: Improved services
945 and an expanding collection of metabolites. Nucleic Acids Res 44:D1214-9.
946 113. Murail S, de Vries SJ, Rey J, Moroy G, Tufféry P. 2021. SeamDock: An Interactive
947 and Collaborative Online Docking Resource to Assist Small Compound
948 Molecular Docking. Front Mol Biosci 8:716466.

114. Felsenstein J. 1985. CONFIDENCE LIMITS ON PHYLOGENIES: AN APPROACH USING THE BOOTSTRAP. Evolution 39:783-791.

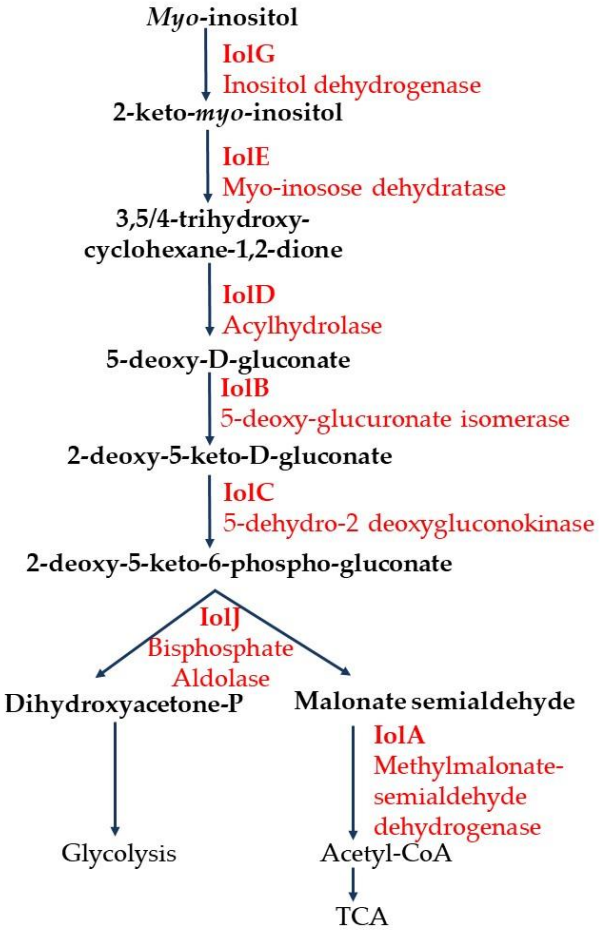
Myo-inositol
IolG
Inositol dehydrogenase
2-keto-*myo*-inositol
IolE
Myo-inosose dehydratase
3,5/4-trihydroxy-
cyclohexane-1,2-dione
IolD
Acylhydrolase
5-deoxy-D-gluconate
IolB
5-deoxy-glucuronate isomerase
2-deoxy-5-keto-D-gluconate
IolC
5-dehydro-2 deoxygluconokinase
2-deoxy-5-keto-6-phospho-gluconate
IolJ
Bisphosphate
Aldolase
Dihydroxyacetone-P
Malonate semialdehyde
IolA
Methylmalonate-
semialdehyde
dehydrogenase
Glycolysis
Acetyl-CoA
TCA

Fig. 1

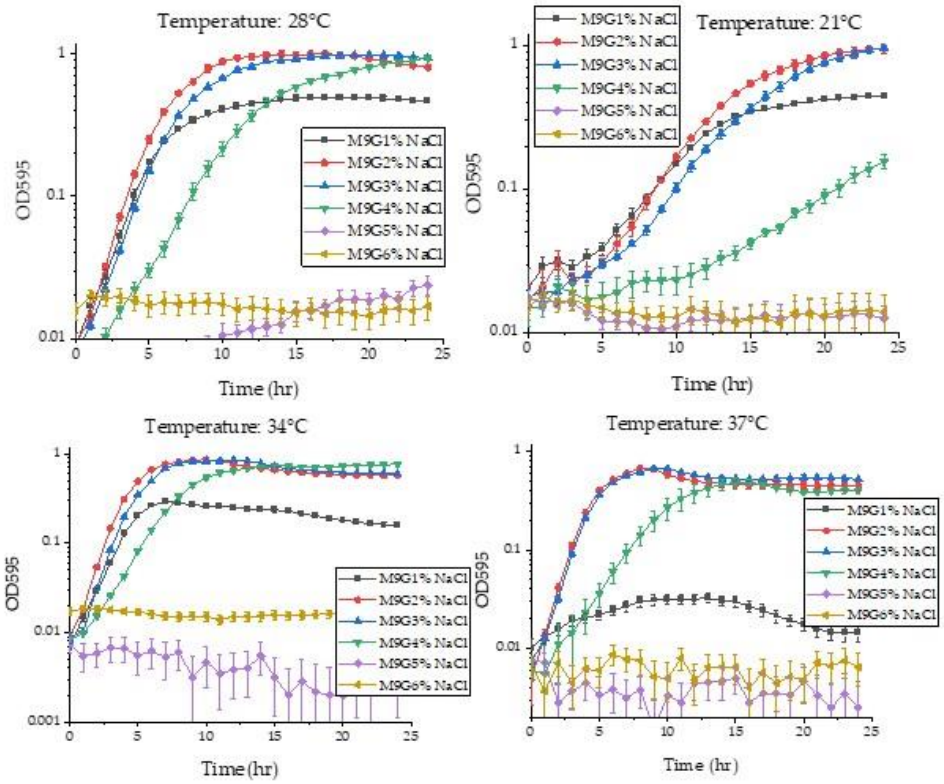
Temperature: 28°C
Temperature: 21°C
Temperature: 34°C
Temperature: 37°C
OD595
Time (hr)
M9G1% NaCl
M9G2% NaCl
M9G3% NaCl
M9G4% NaCl
M9G5% NaCl
M9G6% NaCl

Fig. 2

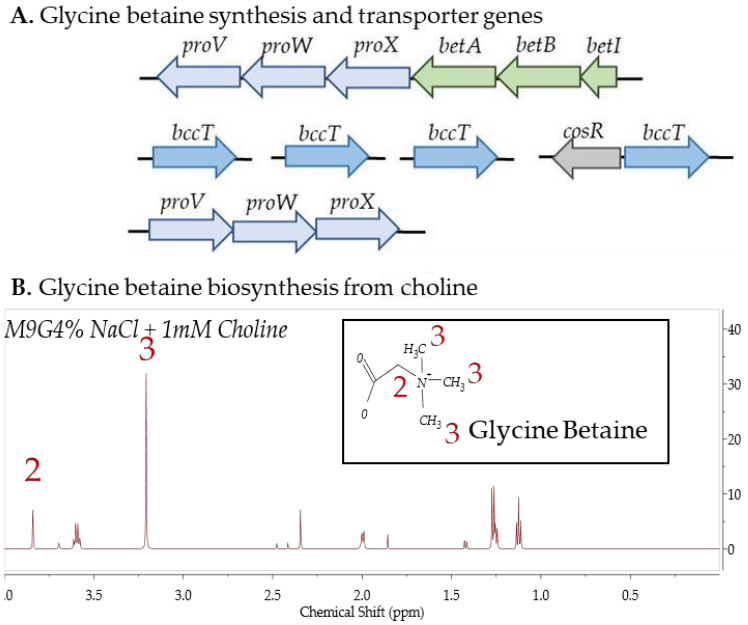
A. Glycine betaine synthesis and transporter genes
proV
proW
proX
betA
betB
betI
bccT
bccT
bccT
cosR
bccT
proV
proW
proX
B. Glycine betaine biosynthesis from choline
M9G4% NaCl + 1mM Choline
3
2
Glycine Betaine
Chemical Shift (ppm)

Fig. 3

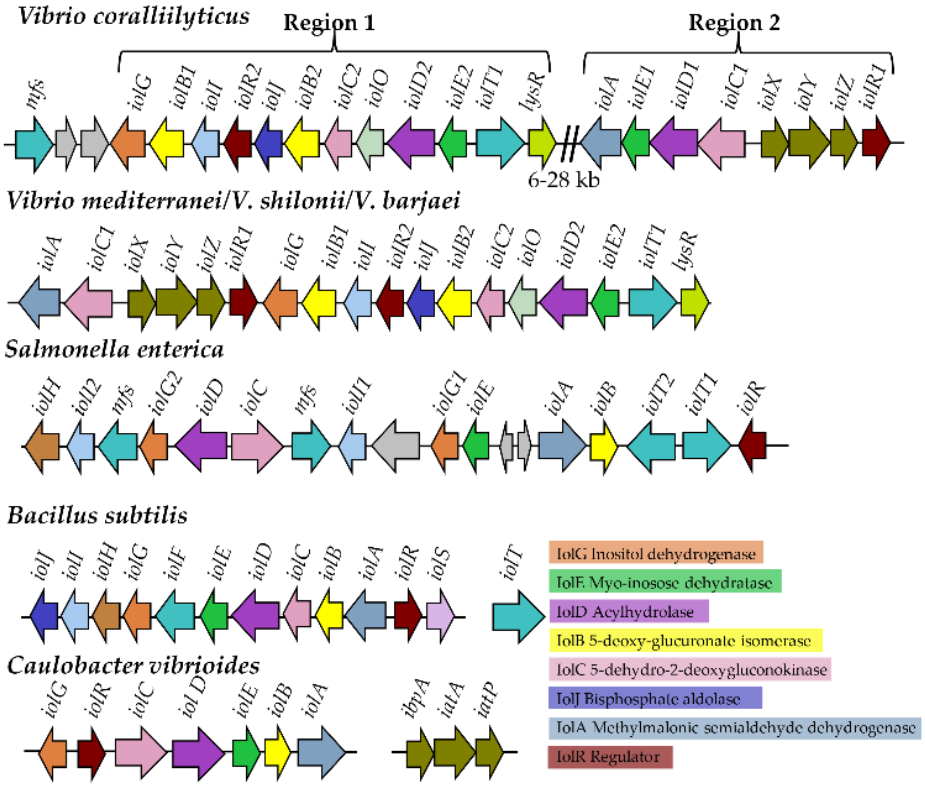
Vibrio coralliilyticus
Region 1
Region 2
mfs
iolG
iolB1
iolI
iolR2
iolJ
iolB2
iolC2
iolO
iolD2
iolE2
iolT1
lysR
iolA
iolE1
iolD1
iolC1
iolX
iolY
iolZ
iolR1
6-28 kb
Vibrio mediterranei/V. shilonii/V. barjaei
iolA
iolC1
iolX
iolY
iolZ
iolR1
iolG
iolB1
iolI
iolR2
iolJ
iolB2
iolC2
iolO
iolD2
iolE2
iolT1
lysR
Salmonella enterica
iolH
iolI2
mfs
iolG2
iolD
iolC
mfs
iolI1
iolG1
iolE
iolA
iolB
iolT2
iolT1
iolR
Bacillus subtilis
iolJ
iolI
iolH
iolG
iolF
iolE
iolD
iolC
iolB
iolA
iolR
iolS
iolT
Caulobacter vibrioides
iolG
iolR
iolC
iol D
iolE
iolB
iolA
iupA
iatA
iatP
IolG Inositol dehydrogenase
IolF Myo-inosose dehydratase
IolD Acylhydrolase
IolB 5-deoxy-glucuronate isomerase
IolC 5-dehydro-2-deoxygluconokinase
IolJ Bisphosphate aldolase
IolA Methylmalonic semialdehyde dehydrogenase
IolR Regulator

Fig. 4

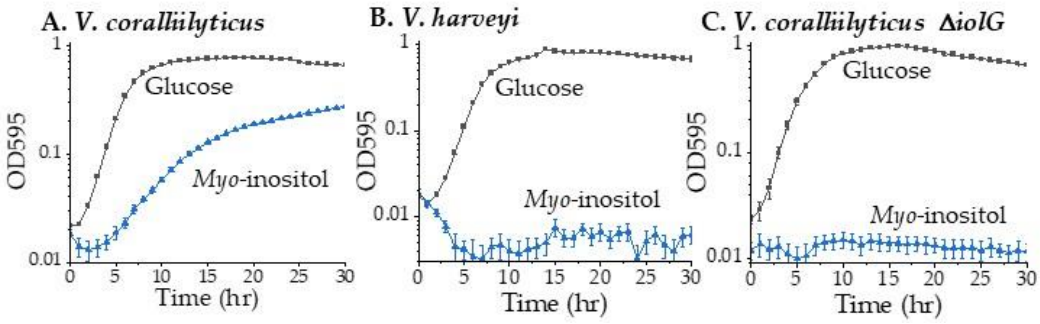

Fig. 5. *V. coralliilyticus* can utilize *myo*-inositol as a sole carbon source. Growth curve analysis in minimal media (M9) containing either 20 mM Glucose (black squares) or 20mM *myo*-inositol (blue triangles). **A.** *V. coralliilyticus* CN52H-1 **B.** *V. harveyi* 393 **C.** *V. coralliilyticus* Δ*iolG.* Growth was measured every hour for 30 h at 28°C. Mean and standard deviation of two biological replicates are shown.

Fig. 5

A. Predicted *myo*-inositol ligand docking in IolT1 (MFS-type transporter)

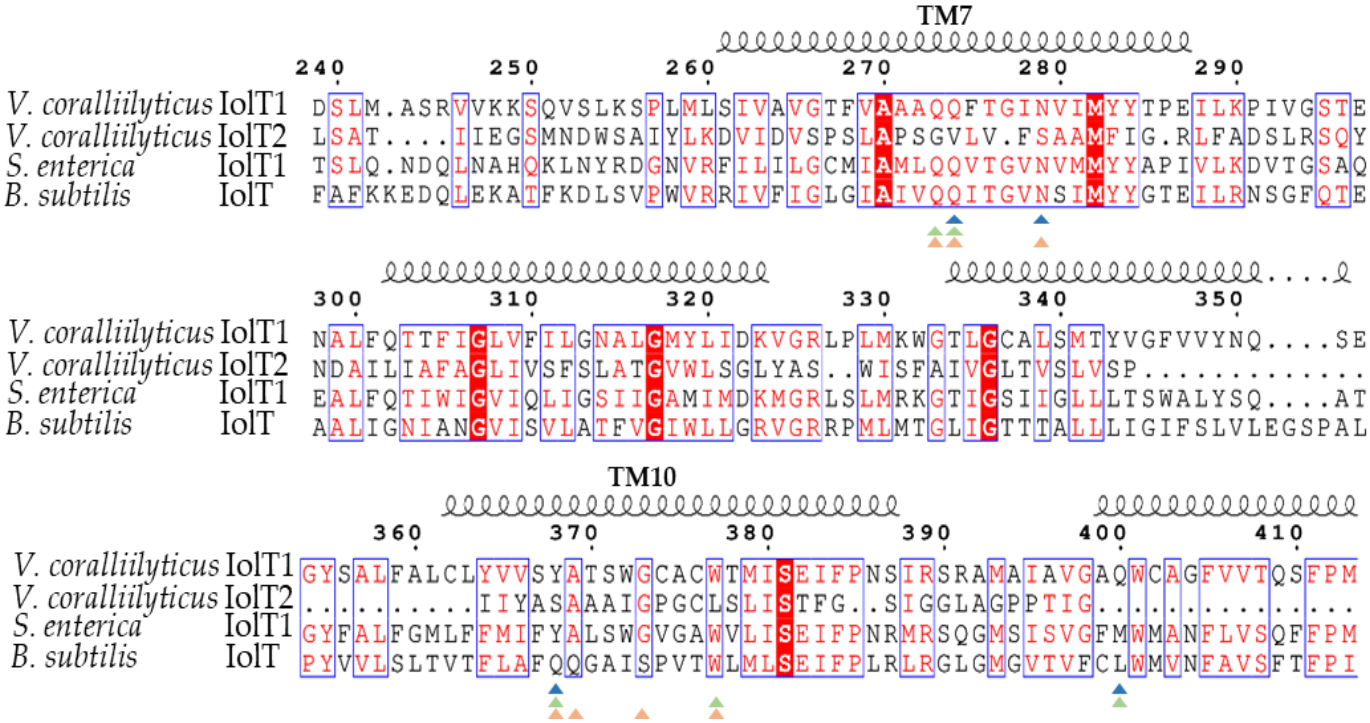

B. Predicted *myo*-inositol ligand docking in IolX (ABC-type transporter)

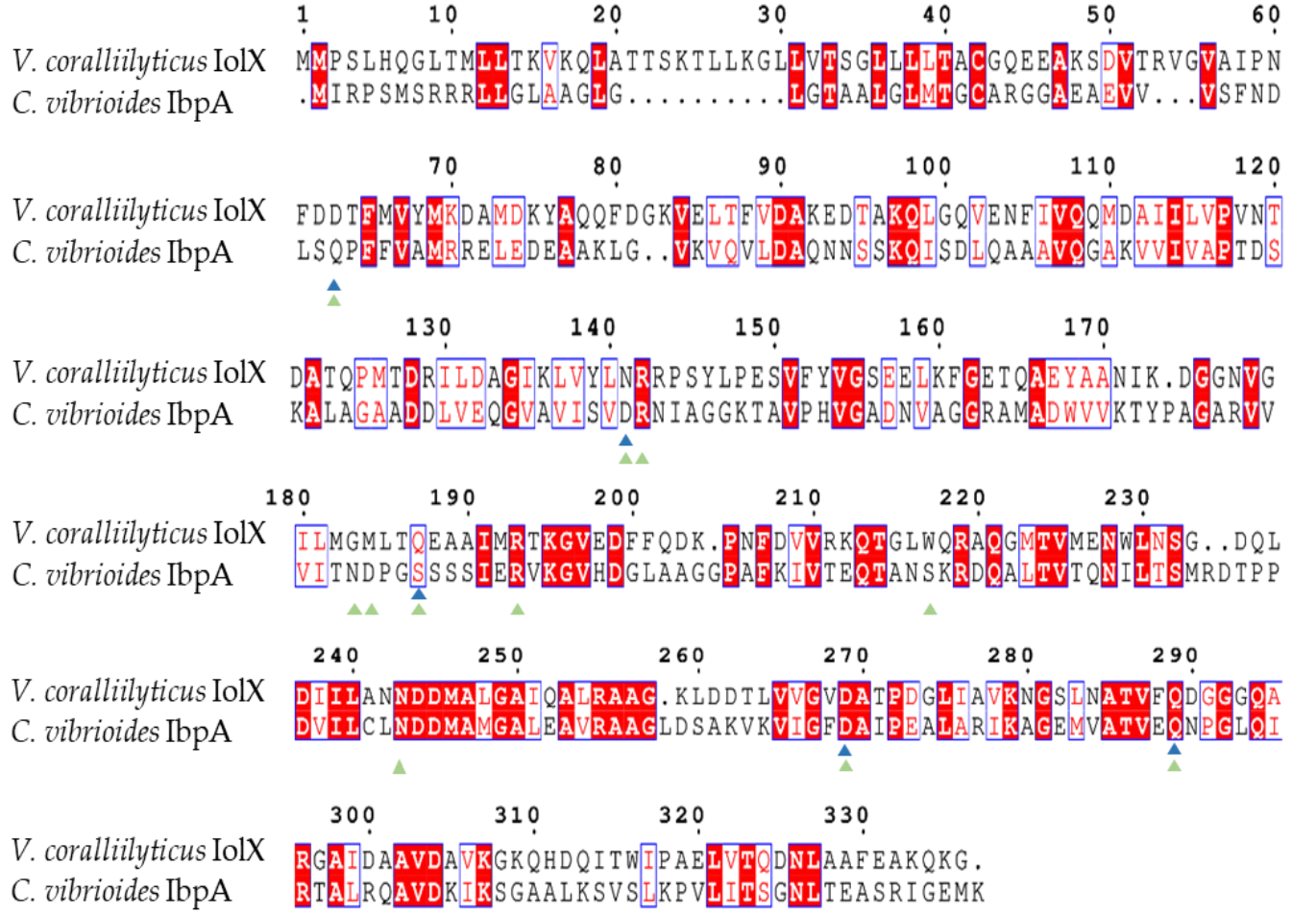

Fig. 6

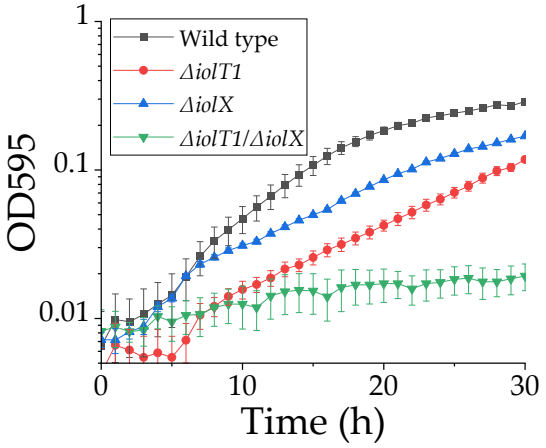

Fig. 7. Growth pattern analysis of transporter deletion mutants. Growth analysis of wild type, Δ*iolT1*, Δ*iolX*, and Δ*iolT1*/ Δ*iolX*. In minimal media (M9G) with 20 mM *myo*-inositol as a sole carbon source. Growth was measured every hour for 30 h at 28°C. Mean and standard deviation of two biological replicates are shown.

Fig. 7

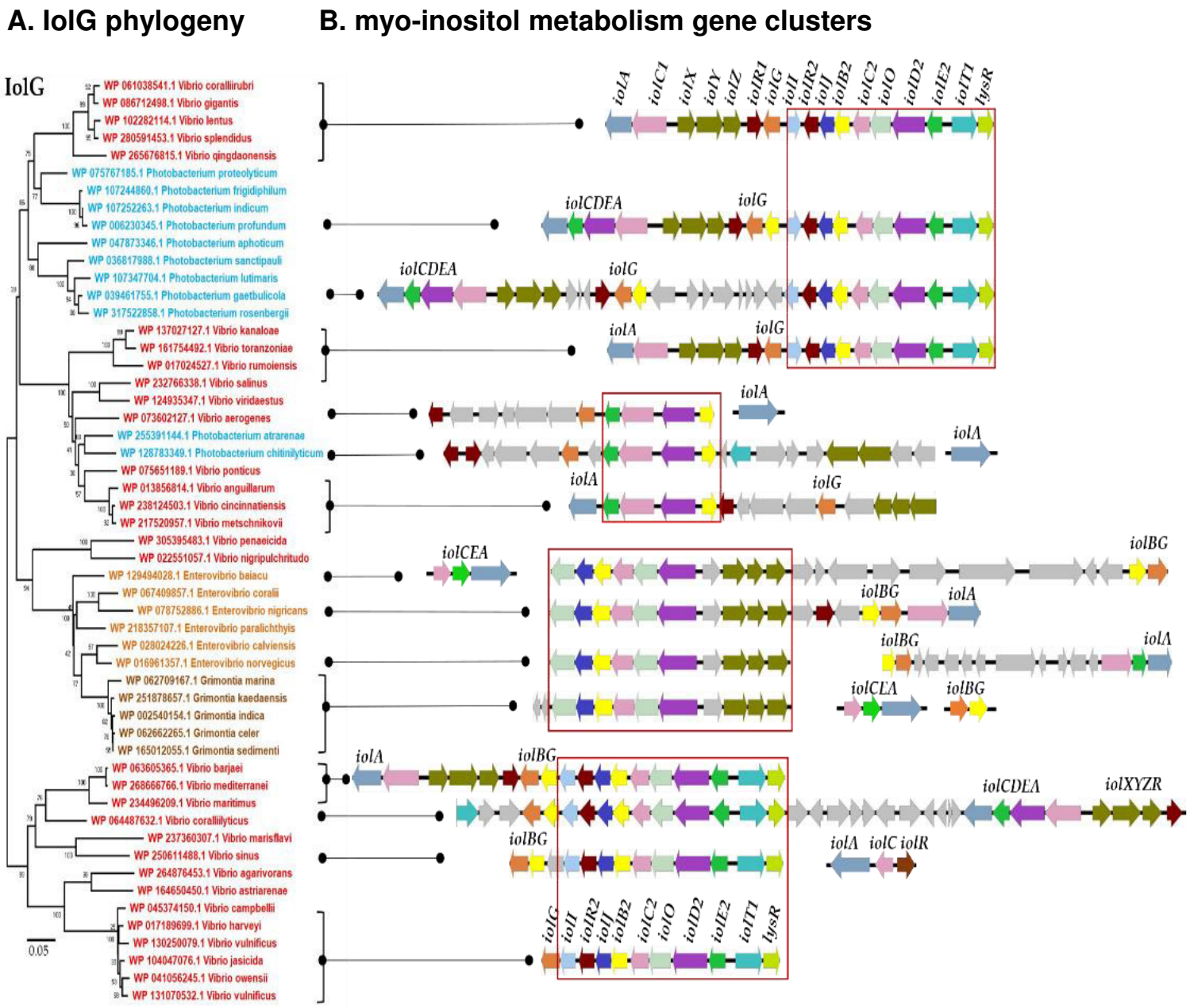
A. IolG phylogeny
B. myo-inositol metabolism gene clusters
IolG
WP 061038541.1 Vibrio coralliirubri
WP 086712498.1 Vibrio gigantis
WP 102282114.1 Vibrio lentus
WP 280591453.1 Vibrio splendidus
WP 265676815.1 Vibrio qingdaonensis
WP 075767185.1 Photobacterium proteolyticum
WP 107244860.1 Photobacterium frigidiphilum
WP 107252263.1 Photobacterium indicum
WP 006230345.1 Photobacterium profundum
WP 047873346.1 Photobacterium aphoticum
WP 036817988.1 Photobacterium sanctipauli
WP 107347704.1 Photobacterium lutimaris
WP 039461755.1 Photobacterium gaetbulicola
WP 317522858.1 Photobacterium rosenbergii
WP 137027127.1 Vibrio kanaloae
WP 161754492.1 Vibrio toranzoniae
WP 017024527.1 Vibrio rumoiensis
WP 232766338.1 Vibrio salinus
WP 124935347.1 Vibrio viridaestus
WP 073602127.1 Vibrio aerogenes
WP 255391144.1 Photobacterium atrarenae
WP 128783349.1 Photobacterium chitinilyticum
WP 075651189.1 Vibrio ponticus
WP 013856814.1 Vibrio anguillarum
WP 238124503.1 Vibrio cincinnatiensis
WP 217520957.1 Vibrio metschnikovii
WP 305395483.1 Vibrio penaeicida
WP 022551057.1 Vibrio nigripulchritudo
WP 129494028.1 Enterovibrio baiacu
WP 067409857.1 Enterovibrio coralii
WP 078752886.1 Enterovibrio nigricans
WP 218357107.1 Enterovibrio paralichthyis
WP 028024226.1 Enterovibrio calviensis
WP 016961357.1 Enterovibrio norvegicus
WP 062709167.1 Grimontia marina
WP 251878657.1 Grimontia kaedaensis
WP 002540154.1 Grimontia indica
WP 062662265.1 Grimontia celer
WP 165012055.1 Grimontia sedimenti
WP 063605365.1 Vibrio barjaei
WP 268666766.1 Vibrio mediterranei
WP 234496209.1 Vibrio maritimus
WP 064487632.1 Vibrio coralliilyticus
WP 237360307.1 Vibrio marisflavi
WP 250611488.1 Vibrio sinus
WP 264876453.1 Vibrio agarivorans
WP 164650450.1 Vibrio astriarenae
WP 045374150.1 Vibrio campbellii
WP 017189699.1 Vibrio harveyi
WP 130250079.1 Vibrio vulnificus
WP 104047076.1 Vibrio jasicida
WP 041056245.1 Vibrio owensii
WP 131070532.1 Vibrio vulnificus
0.05
iolA iolC1 iolX iolY iolZ iolR1 iolG iolI iolR2 iolJ iolB2 iolC2 iolO iolD2 iolE2 iolT1 lysR
iolCDEA iolG
iolCDEA iolG
iolA iolG
iolA
iolA
iolA iolG
iolCEA
iolBG
iolBG iolA
iolBG iolA
iolCEA iolBG
iolA iolBG
iolCDEA iolXYZR
iolBG
iolA iolC iolR
iolG iolI iolR2 iolJ iolB2 iolC2 iolO iolD2 iolE2 iolT1 lysR

Fig. 8

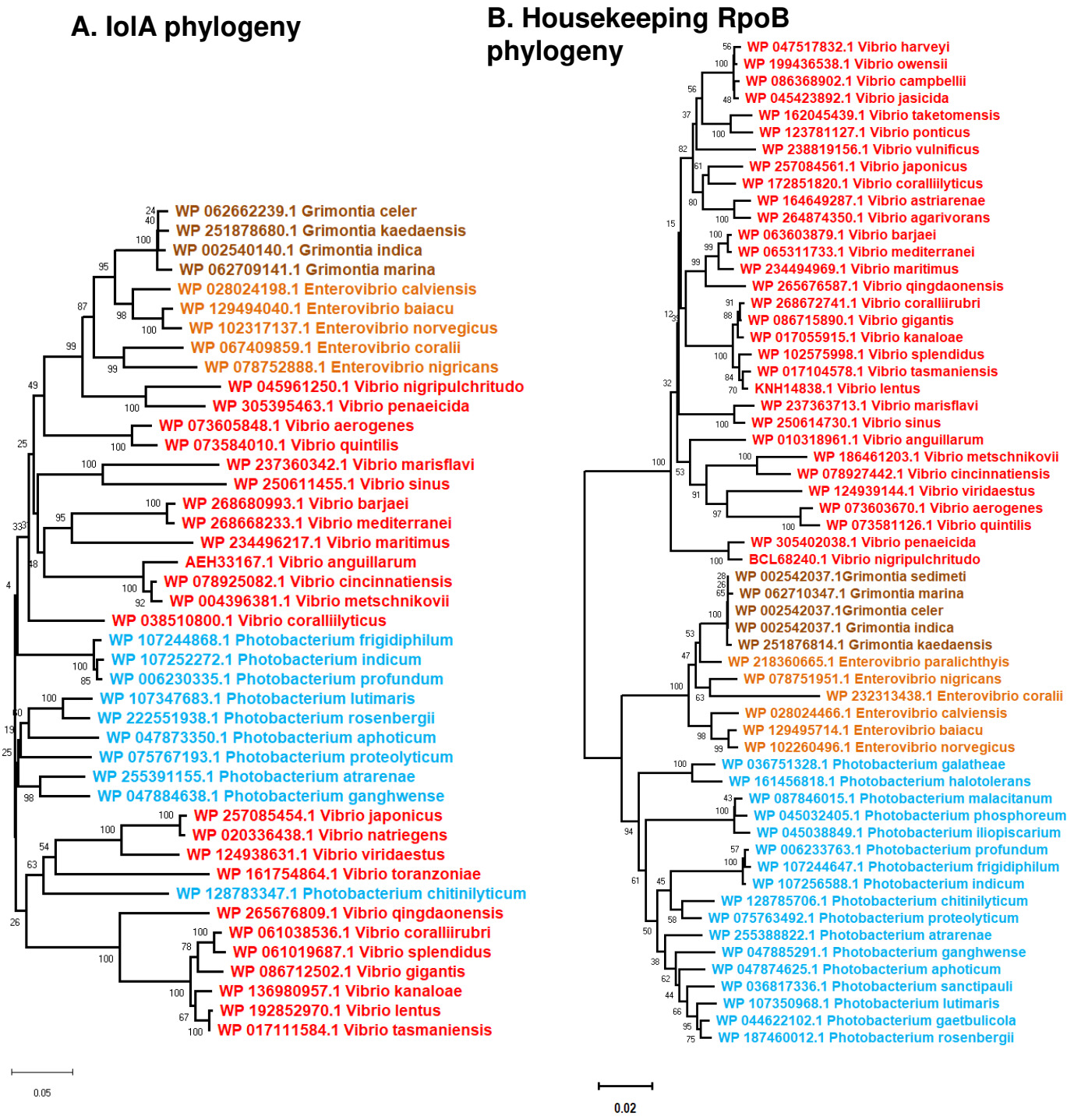
A. IolA phylogeny
WP 062662239.1 Grimontia celer
WP 251878680.1 Grimontia kaedaensis
WP 002540140.1 Grimontia indica
WP 062709141.1 Grimontia marina
WP 028024198.1 Enterovibrio calviensis
WP 129494040.1 Enterovibrio baiacu
WP 102317137.1 Enterovibrio norvegicus
WP 067409859.1 Enterovibrio coralii
WP 078752888.1 Enterovibrio nigricans
WP 045961250.1 Vibrio nigripulchritudo
WP 305395463.1 Vibrio penaeicida
WP 073605848.1 Vibrio aerogenes
WP 073584010.1 Vibrio quintilis
WP 237360342.1 Vibrio marisflavi
WP 250611455.1 Vibrio sinus
WP 268680993.1 Vibrio barjaei
WP 268668233.1 Vibrio mediterranei
WP 234496217.1 Vibrio maritimus
AEH33167.1 Vibrio anguillarum
WP 078925082.1 Vibrio cincinnatiensis
WP 004396381.1 Vibrio metschnikovii
WP 038510800.1 Vibrio coralliilyticus
WP 107244868.1 Photobacterium frigidiphilum
WP 107252272.1 Photobacterium indicum
WP 006230335.1 Photobacterium profundum
WP 107347683.1 Photobacterium lutimaris
WP 222551938.1 Photobacterium rosenbergii
WP 047873350.1 Photobacterium aphoticum
WP 075767193.1 Photobacterium proteolyticum
WP 255391155.1 Photobacterium atrarenae
WP 047884638.1 Photobacterium ganghwense
WP 257085454.1 Vibrio japonicus
WP 020336438.1 Vibrio natriegens
WP 124938631.1 Vibrio viridaestus
WP 161754864.1 Vibrio toranzoniae
WP 128783347.1 Photobacterium chitinilyticum
WP 265676809.1 Vibrio qingdaonensis
WP 061038536.1 Vibrio coralliirubri
WP 061019687.1 Vibrio splendidus
WP 086712502.1 Vibrio gigantis
WP 136980957.1 Vibrio kanaloae
WP 192852970.1 Vibrio lentus
WP 017111584.1 Vibrio tasmaniensis
0.05
B. Housekeeping RpoB phylogeny
WP 047517832.1 Vibrio harveyi
WP 199436538.1 Vibrio owensii
WP 086368902.1 Vibrio campbellii
WP 045423892.1 Vibrio jasicida
WP 162045439.1 Vibrio taketomensis
WP 123781127.1 Vibrio ponticus
WP 238819156.1 Vibrio vulnificus
WP 257084561.1 Vibrio japonicus
WP 172851820.1 Vibrio coralliilyticus
WP 164649287.1 Vibrio astriarenae
WP 264874350.1 Vibrio agarivorans
WP 063603879.1 Vibrio barjaei
WP 065311733.1 Vibrio mediterranei
WP 234494969.1 Vibrio maritimus
WP 265676587.1 Vibrio qingdaonensis
WP 268672741.1 Vibrio coralliirubri
WP 086715890.1 Vibrio gigantis
WP 017055915.1 Vibrio kanaloae
WP 102575998.1 Vibrio splendidus
WP 017104578.1 Vibrio tasmaniensis
KNH14838.1 Vibrio lentus
WP 237363713.1 Vibrio marisflavi
WP 250614730.1 Vibrio sinus
WP 010318961.1 Vibrio anguillarum
WP 186461203.1 Vibrio metschnikovii
WP 078927442.1 Vibrio cincinnatiensis
WP 124939144.1 Vibrio viridaestus
WP 073603670.1 Vibrio aerogenes
WP 073581126.1 Vibrio quintilis
WP 305402038.1 Vibrio penaeicida
BCL68240.1 Vibrio nigripulchritudo
WP 002542037.1Grimontia sedimeti
WP 062710347.1 Grimontia marina
WP 002542037.1Grimontia celer
WP 002542037.1 Grimontia indica
WP 251876814.1 Grimontia kaedaensis
WP 218360665.1 Enterovibrio paralichthyis
WP 078751951.1 Enterovibrio nigricans
WP 232313438.1 Enterovibrio coralii
WP 028024466.1 Enterovibrio calviensis
WP 129495714.1 Enterovibrio baiacu
WP 102260496.1 Enterovibrio norvegicus
WP 036751328.1 Photobacterium galatheae
WP 161456818.1 Photobacterium halotolerans
WP 087846015.1 Photobacterium malacitanum
WP 045032405.1 Photobacterium phosphoreum
WP 045038849.1 Photobacterium iliopiscarium
WP 006233763.1 Photobacterium profundum
WP 107244647.1 Photobacterium frigidiphilum
WP 107256588.1 Photobacterium indicum
WP 128785706.1 Photobacterium chitinilyticum
WP 075763492.1 Photobacterium proteolyticum
WP 255388822.1 Photobacterium atrarenae
WP 047885291.1 Photobacterium ganghwense
WP 047874625.1 Photobacterium aphoticum
WP 036817336.1 Photobacterium sanctipauli
WP 107350968.1 Photobacterium lutimaris
WP 044622102.1 Photobacterium gaetbulicola
WP 187460012.1 Photobacterium rosenbergii
0.02

Fig. 9

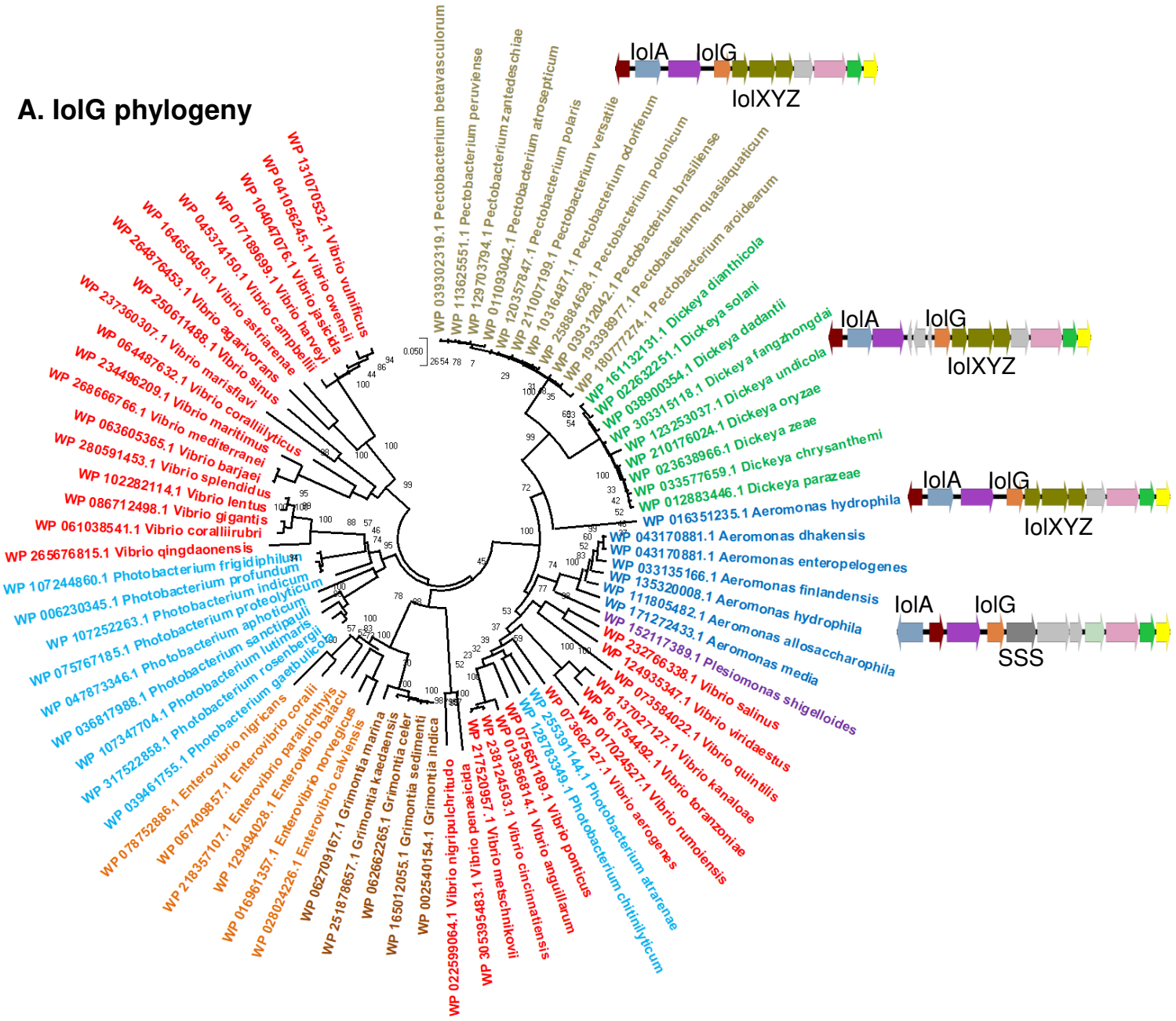
A. IolG phylogeny
IolA
IolG
IolXYZ
SSS
WP 039302319.1 Pectobacterium betavasculorum
WP 113625551.1 Pectobacterium peruviense
WP 129703794.1 Pectobacterium zantedeschiae
WP 011093042.1 Pectobacterium atrosepticum
WP 120357847.1 Pectobacterium polaris
WP 211007199.1 Pectobacterium versatile
WP 103164871.1 Pectobacterium odoriferum
WP 258884628.1 Pectobacterium polonicum
WP 039312042.1 Pectobacterium brasiliense
WP 193398977.1 Pectobacterium quasiaquaticum
WP 180777274.1 Pectobacterium aroidearum
WP 161132131.1 Dickeya dianthicola
WP 022632251.1 Dickeya solani
WP 038900354.1 Dickeya dadantii
WP 303315118.1 Dickeya fangzhongdai
WP 123253037.1 Dickeya undicola
WP 210176024.1 Dickeya oryzae
WP 023638966.1 Dickeya zeae
WP 033577659.1 Dickeya chrysanthemi
WP 012883446.1 Dickeya parazeae
WP 016351235.1 Aeromonas hydrophila
WP 043170881.1 Aeromonas dhakensis
WP 043170881.1 Aeromonas enteropelogenes
WP 033135166.1 Aeromonas finlandensis
WP 135320008.1 Aeromonas hydrophila
WP 111805482.1 Aeromonas allosaccharophila
WP 171272433.1 Aeromonas media
WP 152117389.1 Plesiomonas shigelloides
WP 232766338.1 Vibrio salinus
WP 124935347.1 Vibrio viridaestus
WP 073584022.1 Vibrio quintilis
WP 137027127.1 Vibrio kanaloae
WP 161754492.1 Vibrio tortanzoniae
WP 017024527.1 Vibrio rumoiensis
WP 073602127.1 Vibrio aerogenes
WP 255391144.1 Photobacterium atrarenae
WP 128783349.1 Photobacterium chitinilyticum
WP 075651189.1 Vibrio ponticus
WP 013856814.1 Vibrio anguillarum
WP 238124503.1 Vibrio cincinnatiensis
WP 217520957.1 Vibrio metschnikovii
WP 305395483.1 Vibrio penaeicida
WP 022599064.1 Vibrio nigripulchritudo
WP 002540154.1 Grimontia indica
WP 165012055.1 Grimontia sedimenti
WP 062662265.1 Grimontia celer
WP 251878657.1 Grimontia kaedaensis
WP 062709167.1 Grimontia marina
WP 028024226.1 Enterovibrio norvegicus
WP 016961357.1 Enterovibrio calviensis
WP 129494028.1 Enterovibrio balacu
WP 218357107.1 Enterovibrio paralichthyis
WP 067409857.1 Enterovibrio coralii
WP 078752886.1 Enterovibrio nigricans
WP 039461755.1 Photobacterium gaetbulicola
WP 317522858.1 Photobacterium rosenbergii
WP 107347704.1 Photobacterium lutimaris
WP 036817988.1 Photobacterium sanctipauli
WP 047873346.1 Photobacterium aphoticum
WP 075767185.1 Photobacterium proteolyticum
WP 107252263.1 Photobacterium indicum
WP 006230345.1 Photobacterium profundum
WP 107244860.1 Photobacterium frigidiphilum
WP 265676815.1 Vibrio qingdaonensis
WP 061038541.1 Vibrio coralliirubri
WP 086712498.1 Vibrio gigantis
WP 102282114.1 Vibrio lentus
WP 280591453.1 Vibrio splendidus
WP 063605365.1 Vibrio barjaei
WP 268666766.1 Vibrio mediterranei
WP 234496209.1 Vibrio maritimus
WP 064487632.1 Vibrio coralliilyticus
WP 237360307.1 Vibrio marisflavi
WP 250611488.1 Vibrio sinus
WP 264876453.1 Vibrio agarivorans
WP 164650450.1 Vibrio astriarenae
WP 045374150.1 Vibrio campbellii
WP 017189699.1 Vibrio harveyi
WP 104047076.1 Vibrio jasicida
WP 041056245.1 Vibrio owensii
WP 131070532.1 Vibrio vulnificus
0.050
B. myo-inositol metabolism gene clusters within mobile genetic elements
Aeromonas hydrophila
tRNA-Leu
phage
IS3
Int
Aeromonas dhakensis
tRNA-ser
HsdRSM
phage
Int
Aeromonas hydrophila WCX23 NZ_CP038463.1
phage
IS5
IS21
T6SS
Int
T6SS
tRNA-His

Fig. 10